The Universe in X-rays:

Overview of HW#1

ATHENA – Advenced Telescope for High ENergy Astrophysics, 2037???

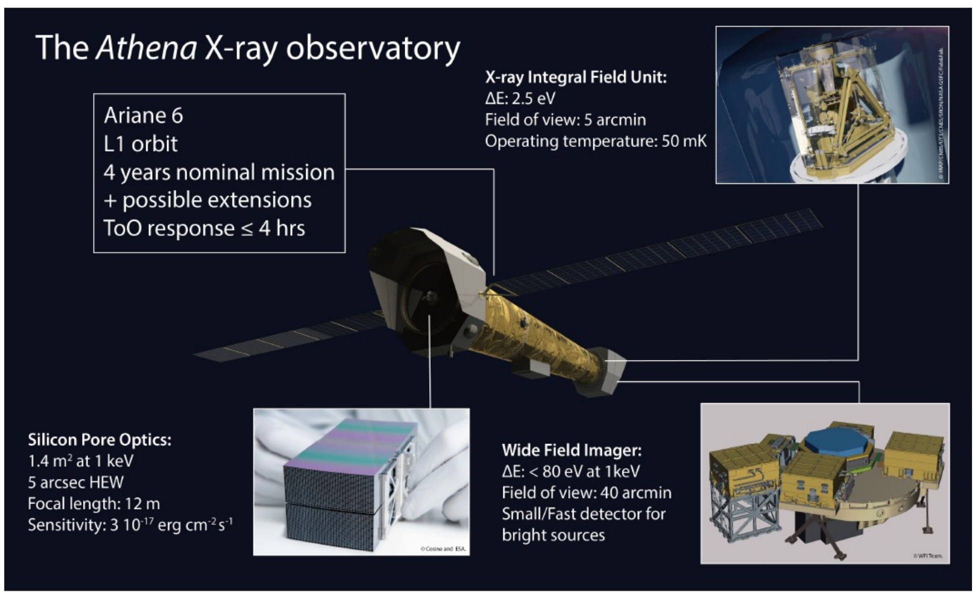

Fundamental questions - ATHENA mission

- How does the **large scale structure** in the Universe form and evolve?
- How do **black hole** grow and help shape the Universe?
- How and when are the **chemical elements** formed?

Athena is an observatory with ~500 projects/year:

- Stars, exoplanets, pulsars, neutron stars, gravitational wave events, galaxies
- Unprecedented **discovery space**

Agata Różańska, fall semester, 2022/23

Missing information: resolutions, sensitivity, science goals

AGILE: X-ray and gamma ray astronomical satellite

Sarthak Choudhary
PhD Student
AstroCeNT
CAMK PAN

Introduction

- Operated by Italian Space Agency
- Launched: 23 April, 2007
- Energy range:
  - Gamma ray (30 MeV- 50 GeV)
  - hard X-ray (18-60 keV)
- Fast gamma-ray alert monitoring system
- independent pipelines :
  - Fast pipeline: generates alert within 0.5–1 hour from the time of the last GRID event acquired in orbit.
  - Slow pipeline: more accurate but the alerts are generated 3–3.5 hours after last GRID event acquired in orbit.

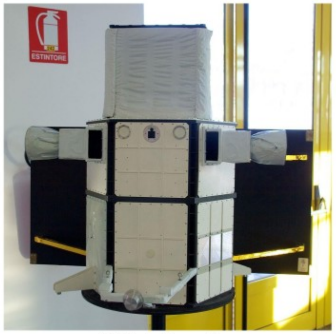

AGILE satellite model
Ref: Wikimedia commons

Instruments

Instrument name: **G**amma **R**ay **I**maging **D**etector (GRID):
Energy range: 30 MeV- 50 GeV

Instrument name: SuperAGILE
It's a coded mask imaging X-ray telescope.
Energy range: 18-60 keV
Detector type: Silicon strip detector

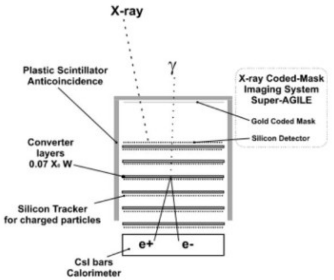

Fig. 1. Description and working principle of the AGILE instrument.

Ref: Astronomy & Astrophysics, 558, A37

References

- https://agile.asdc.asi.it/
- https://en.wikipedia.org/wiki/AGILE_(satellite)
- The AGILE silicon tracker: testbeam results of the prototype silicon detector, 2002NIMPA.490..146B doi.org/10.1016/S0168-9002(02)01062-8

To improve: time resolution, energy resolution, science goals, hard to read figure's text.

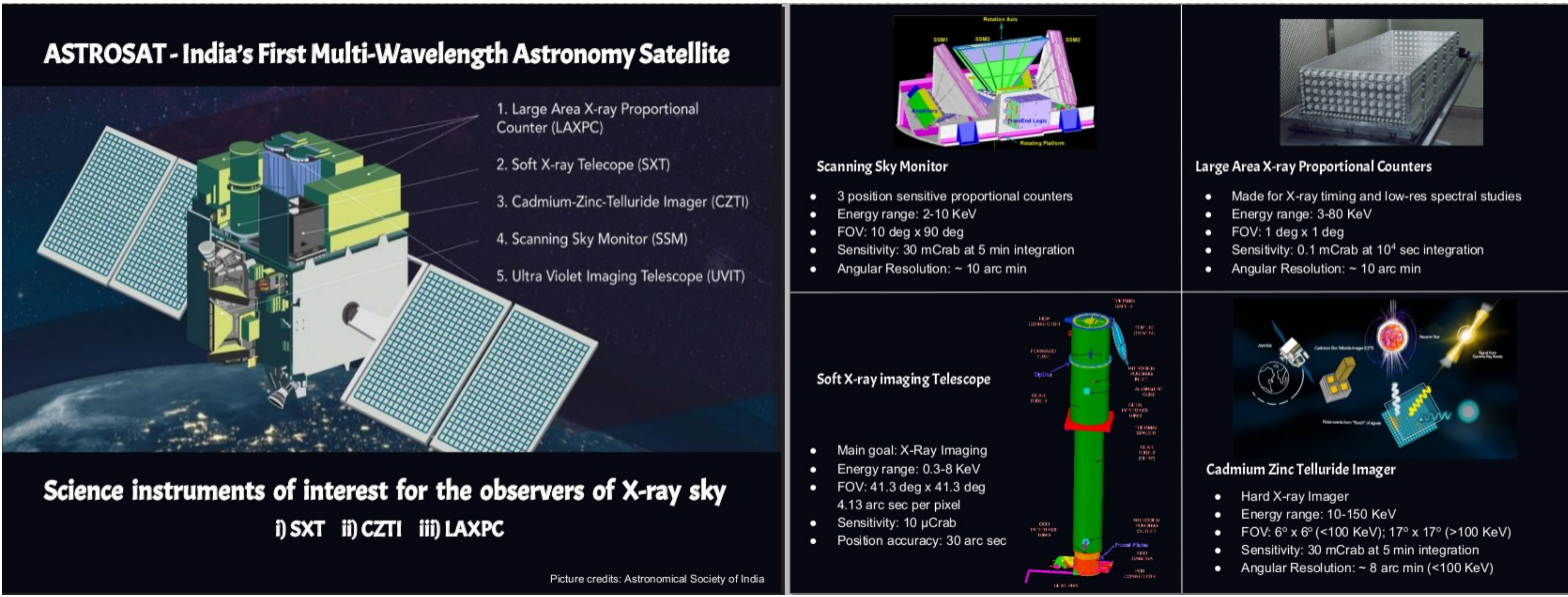

To improve:
time resolution,
energy resolution,
angular resolution,
science goals.

"MAXI" or Monitor of All-Sky X-ray Image

Image source: *NASA*

- Installed on the *International Space station* (ISS) as part of *Japanese Experiment Module Exposed Facility* (JEM-EF or Kibo-EF)
- Energy range of observation: 0.5 - 30 KeV
- Operational from August, 2009 - Present
- Observes the X-ray universe every 92 minutes

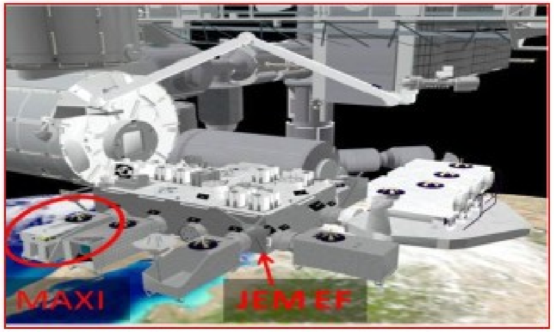

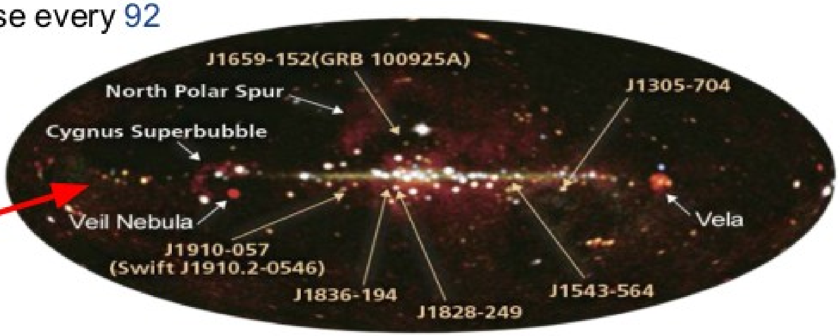

All sky X-ray map by MAXI with four year-exposure showing several individual sources and other x-ray soft structures

Detectors

Image source: *MATSUOKA et al 2009*

Gas Slit Cameras (GSC)

- 1-D position-sensitive gas PC with 10µm carbon anode wires + slit & slat collimators
- Xenon at 1.4 atmospheres with 1% CO_2
- Overall 12 such counters with a total effective area 5350 cm^2
- Operates in 2-30 KeV range

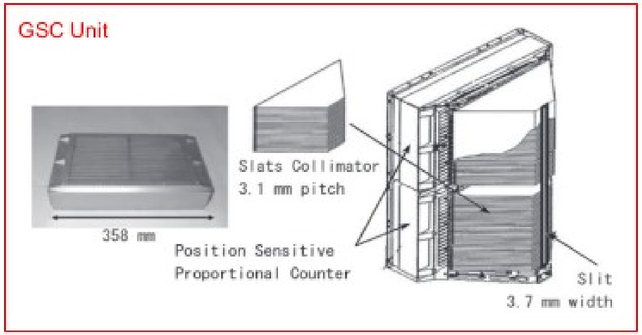

Solid State Slit Camera (SSC)

- Total 32 Peltier-cooled X-ray sensitive CCD chips + slit and slat collimators
- The pixel size is 24x24 µm, and there are total of 1024x1024 pixels.
- Total effective area ~ 200 cm^2
- Operates in 0.5-15 keV range

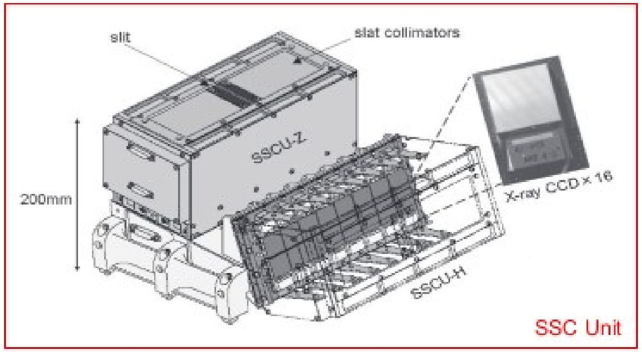

To improve: resolutions, sensitivity, detectors never worked together.

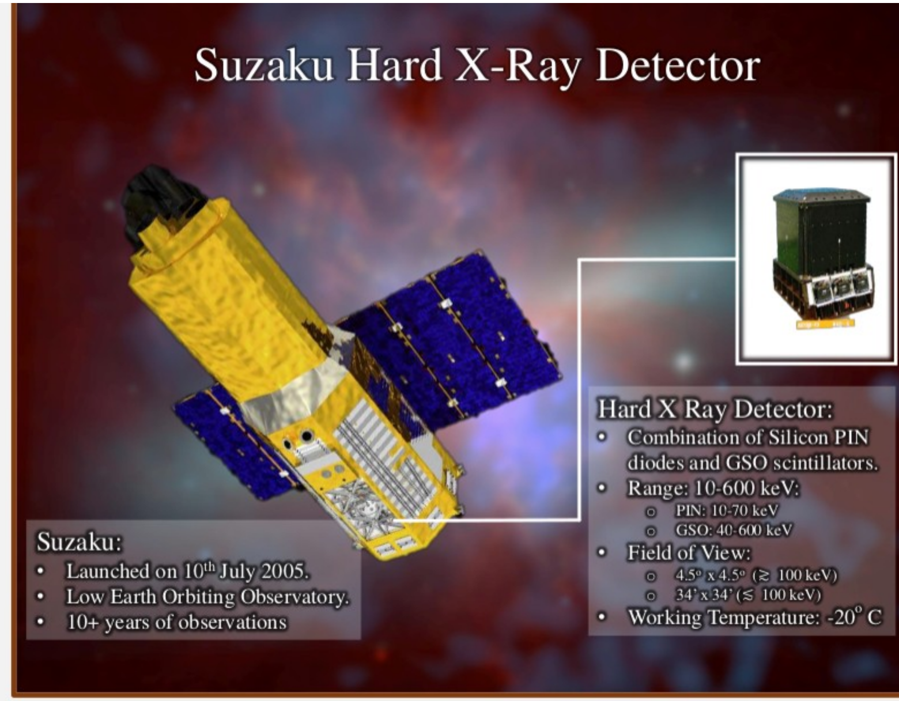

Suzaku-Mission HXD:

- Suzaku (aka Astro-E2) is recovery mission for lost Astro-E mission.
- The HXD installed in Suzaku is similar to Astro-E mission with minor developments in sensors and analogue electronics.
- The HXD is a non imaging **High resolution X-Ray Spectrometer**.
- The HXD was one of the most sensitive instrument (with low background) of that time with a wide observing range.
- Main Aim:
  - **Active Galactic Nuclei Spectra**
  - **Cataclysmic Variables**
  - **Probe Strong Gravity** etc..
- An example of **HXD X-Ray Spectrum** is shown in Figure 1 of the galaxy **Centaurus-A**.

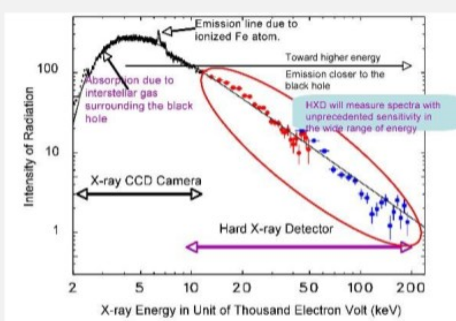

Figure 1: X-Ray Spectrum of Centaurus A. The red points represent the results observed by the Siclicon PIN diode while the blue dots represent the GSO crystal observations.

References:

- Tadayuki Takahashi, *et al* . Hard X-Ray Detector (HXD) on Board Suzaku. Publications of the Astronomical Society of Japan, 59(sp1):S35–S51, 01 2007.
- http://www.astro.isas.jaxa.jp/suzaku/presentation/Download/2005_Einstein_Takahashi.pdf
- http://www.astro.isas.jaxa.jp/suzaku/presentation/Download/suzaku_2006_aas_stellar.pdf

Images Credits:

- Background Image: https://upload.wikimedia.org/wikipedia/commons/8/83/M82_Chandra_HST_Spitzer.jpg
- Suzaku: https://www.isas.jaxa.jp/en/missions/files/suzaku_main.jpg
- HXD: https://heasarc.gsfc.nasa.gov/docs/suzaku/gallery/instruments/hxd.html
- Figure 1: https://heasarc.gsfc.nasa.gov/docs/suzaku/gallery/science/hxd1st.html

To improve: resolutions, sensitivity, put in the context of the whole mission.

CHANDRA Advanced CCD Imaging Spectrometer (ACIS)

Each chip
1024 ✕ 1024 pixels
8′ ✕ 8′ FOV

Maximum six CCD can be ON at a time
Different configurations possible

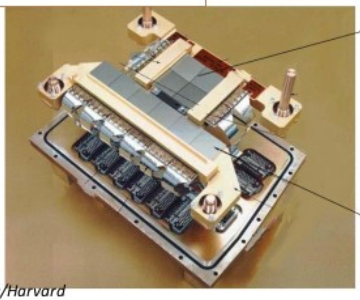

Credits: Chandra/Harvard

4 Imaging Chips

Front Illuminated
Total FOV: 16´ X 16´

6 Spectroscopic chips — Can be used with gratings

4 Front Illuminated
2 Black Illuminated

Maximum read-out-rate per channel ~ 100 kpix/sec
Detector operating temperature −90 to −120°C

Science with ACIS

- Better Sensitivity than previous X-ray missions
- Detailed study of black holes, Supernovae and Dark Matter
- Spectroscopic CCD array with gratings give highest resolutions for detailed study of motions through Doppler line shifts in supernova remnants, X-ray binaries
- Allows detailed study of jets

To improve: mark where is the IBIS, less text.

INTEGRAL IBIS

IBIS: IMAGER ON BOARD THE INTEGRAL SATELLITE

Principal Investigator:
Pietro Ubertini, INAF/IASF-Rome Italy

Co-Principal Investigators:
Philippe Laurent, CEA-Saclay, France
Guido DiCocco, INAF/IASF-Bologna, Italy

with collaborating scientific institutes in Italy (INAF/IASF-Rome, INAF/IASF-Bologna, INAF/IASF-Palermo), France (CEA Saclay), Norway (U Bergen), Germany (U Tübingen), Spain (U Valencia), USA (NASA/MSFC Huntsville), Poland (Space Research Centre, Warsaw), UK (U Southampton).

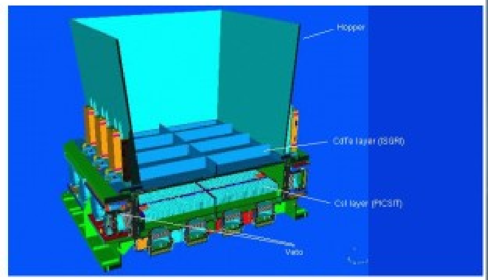

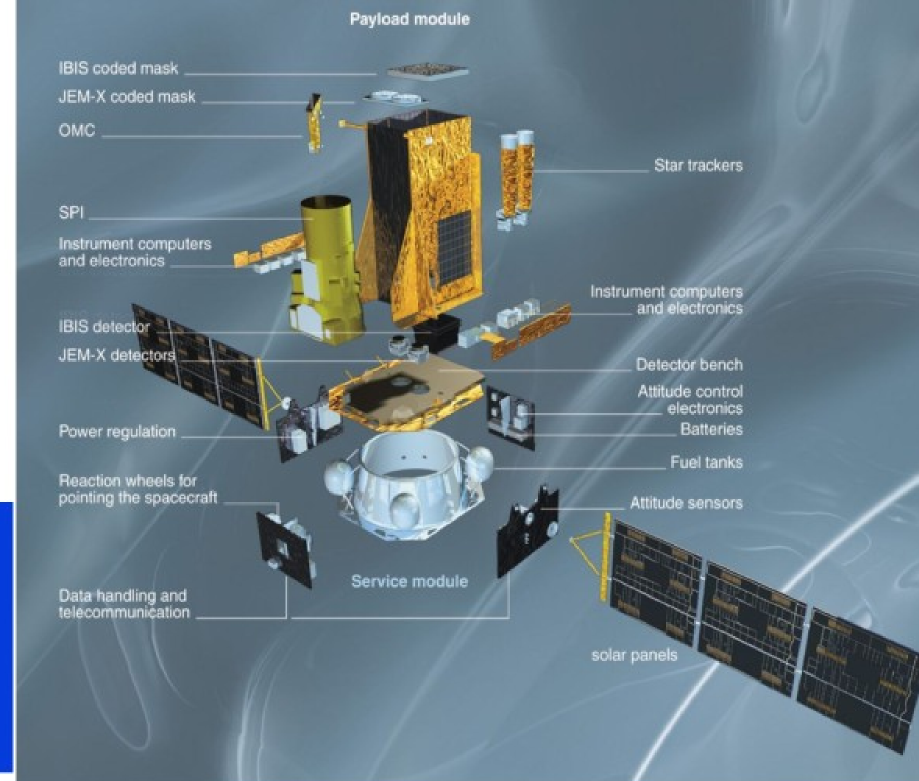

The scientific goals of INTEGRAL are addressed through the use of high resolution spectroscopy with fine imaging and accurate positioning of celestial sources in the gamma-ray domain.

Some of the topics addressed by Integral are:

Compact Objects: White Dwarfs, Neutron Stars, Black Hole Candidates, High Energy Transients

Extragalactic Astronomy: Galaxies, Clusters, AGN, Seyferts, Blazars, Cosmic Diffuse Background

Nucleosynthesis Studies: Hydrostatic Nucleosynthesis (AGB, WR Stars), Explosive Nucleosynthesis (Supernovae, Novae)

The Galactic Centre: Sgr A*, diffuse emission, monitoring the Galactic Centre and Bulge

Gamma-Ray Bursts: Alerts, GRB properties

Classification and Identification of High Energy Sources: Source Catalogues, Identifying Gamma-Ray Objects

PLUS: Unexpected Discoveries (Obscured sources, Supergiant Fast X-ray Transients, hard tails from magnetars)

OVERVIEW OF SCIENTIFIC CAPABILITIES OF IBIS

Energy range	15 keV - 10 MeV
Detector area	2600 cm^2 (CdTe - Cadmium Telluride) 3000 cm^2 (CsI - Caesium Iodide)
Spectral energy resolution (FWHM)	8% @ 100 keV 10% @ 1 MeV
Field of view	8.3° x 8.0° (fully coded) 29.1° x 29.4° (down to zero response)
Angular resolution	12' FWHM
Point source location accuracy (90% error radius)	30" @ 100 keV (50σ source) 3' @ 100 keV (5σ source) 5-10' @ 1 MeV (5σ source)
Continuum sensitivity*	2.85e-6 ph/(s cm^2 keV) [3σ in 10e5 s, @ 100 keV, ΔE = E/2] 1.6e-6 ph/(s cm^2 keV) [3σ in 10e5 s, @1 MeV, ΔE = E/2]
Line sensitivity*	1.9e-5 ph/(s cm^2 [3σ in 10e6 s, @ 100 keV] 3.8e10-4 ph/(s cm^2 [3σ in 10e6 s, @ 1 MeV]
Timing accuracy	61 µs - 1 hr
Typical source location	30" @ 100 keV (50 sigma source) 3' @ 100 keV (5 sigma source)
Resources (following EID-A allocation):	
Mass	677 kg (+ 96 kg for tube inside PLM)
Power (sun/eclipse)	240/0 W
Data rate (solar maximum)	59.8 kbps
Date rate (solar minimum)	56.8 kbp

* The sensitivities are based on in-flight background measurements.

To improve:
time and
angular resolution,
clear science goal.

Scientific goal: survey the distribution of hot gas in the Milky Way and constrain the mass and geometry of the Galactic **halo**.

- A small satellite launched and operated by University of Iowa as part of ISS supply mission
- The observing strategy was to divide the sky into 334 positions and acquire a minimum of 8000 detector-seconds for each position.
- Operating from October 15, 2018, up to September 29, 2020, effectively **doubling the mission life time.**

a non-focusing instrument, comprised of **three independent silicon drift detectors**

- Energy range : 0.4–7.0 keV
- Field of view : 10 deg diameter
- Energy Resolution : ~85 eV at 677 eV and ~137 eV at 5895 eV.

HaloSat

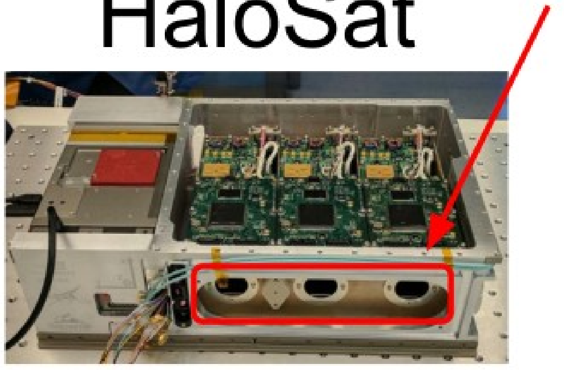

HaloSat - without its top cover

HaloSat and ISS

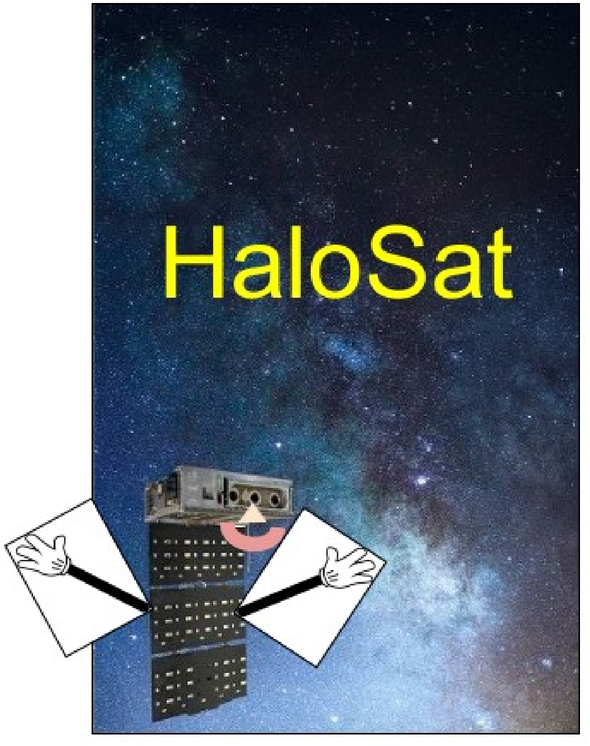

HaloSat in space - artistic vision

To improve:
time and
angular resolution
not for all
instruments,
but I agree it was
hard,
clear science goal
in the form of
questions.

HITOMI

By
Christian Eze
CAMK PAN

Soft X-ray Spectrometer (SXS):
2 componenents (X-ray telescope, SXT-a lightweight mirror and X-ray calorimeter, XCS). XCS is a 6x6 array, has non-dispersive 7 eV resolution in the 0.3-10 keV bandpass with FOV of 3'.

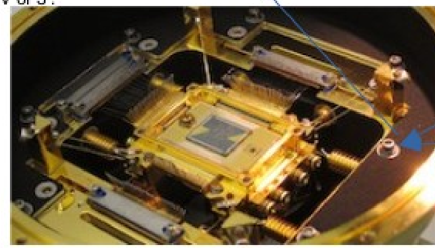

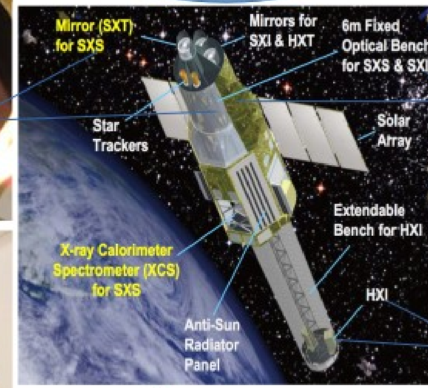

Soft X-ray Imager (SXI):
- a 6-m focal length imaging mirror with a diamter of about 45cm and a CCD camera with next generation Hamamatsu CCD chips. It also has a cooler, an improved quantum efficiency and an optimized response for higher energies.

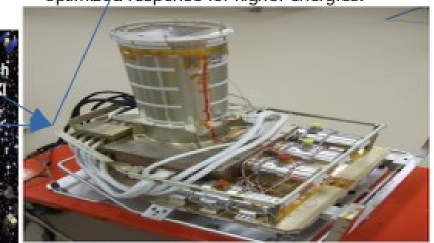

Soft Gamma-ray Detector (SGD): a non-focusing hard X-ray detector with a 50-600 keV energy range and sensitivity at 100 keV, about 10 times better than the Suzaku HXD

- JAXA H-IIA
- Low earth orbit
- Energy range: 0.3-600keV
- 4 instruments: SXS, SXI, HXI, SGD
- Launched on Feb. 17, 2016
- Lost contact with earth on March 27, 2016

Hard X-ray Imager (HXI): 2 identical mirror-detector pairs (an 5-80 keV energy range). The detector is a hybrid double sided silicon strip (DSSD) CdTe pixel array. 9 arcmin x 9 arcmin FOV, spectral resolution of 1 keV at 60 keV, and timing accuracy of < 10msec; operated at 20Â±5C.

Image credit: https://heasarc.gsfc.nasa.gov/docs/hitomi/gallery/instr_gallery.html

Hitomi mission objectives

A. Study of the structure of the universe

How do black hole develop, and how do they impact the surroundings ?

How are galaxy clusters created and how do they evolve ?

When were heavy elements in the universe created , and how much ?

B. Study of the physics in extreme conditions

What physical phenomena are occurring in extreme conditions with high density and strong magnetic fields?

Is space time really distorted near black holes?

Where and how are cosmic rays created?

To improve:
science goal.

JEM–X

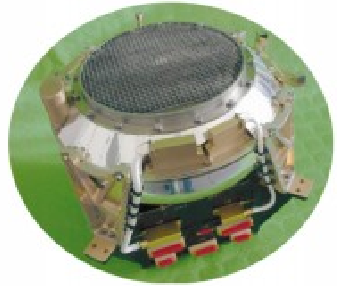

Complete JEM-X unit (image: *JEM-X: The X-ray monitor aboard INTEGRAL*, N. Lund et al.)

INTEGRAL is dedicated to the detailed studies of celestial objects in the gamma ray region. The primary role of **JEM-X** on INTEGRAL is to **extend the energy range** covered by the gamma-ray instruments from their thresholds of 20 to 30 keV downward to about **3 keV**.

JEM–X (Joint European X-Ray Monitor) is a coded aperture instrument consisting of two identical, coaligned telescopes. The baseline photon detection system consists of two high pressure **imaging microstrip gas chambers** (90% Xenon + 10% Methane, 1.5 bar). Each detector unit views the sky through its **coded aperture mask** located at a distance of 3.2 m above the detection plane. The **collimators** limit the Field-of-View (FOV) and act as a supports for the thin beryllium windows against the internal pressure of the detectors . Data acquisition is carried out by **readout chains** (RC Boards).

sources

https://heasarc.gsfc.nasa.gov/docs/integral/integralgof.html

N. Lund et al 1998 Phys. Scr. 1998 39 Physica Scripta *JEM-X: Joint European X-Ray Monitor*

N. Lund et al A&A Volume 411, Number 1, November III 2003 *JEM-X: The X-ray monitor aboard INTEGRAL*

Main characteristics and performance parameters

Timeframe	Launched in October of 2002 and still working.
Energy range	3 - 35 keV
Energy resolution	1.3 keV @ 10 keV $\frac{\Delta E}{E} = 0.40 \cdot \left(\frac{1}{E[\mathrm{keV}]} + \frac{1}{60}\right)^{1/2}$
Angular resolution	3 arcminute
Field of view (diameter)	4.8° fully coded FOV
Continuum sensitivity (3σ in 10^5 s, @ 6 keV)	1.2 x E-4 ph/(s cm² keV)
Line sensitivity (3σ in 10^5 s, @ 6 keV)	1.6 x E-4 ph/(s cm²)
Timing accuracy (3σ)	122 μs
Source location (15σ isolated source)	< 1' (90% confidence)
Mask diameter	535 mm
Detector diameter	250 mm
Mask–detector distance	3 401 mm

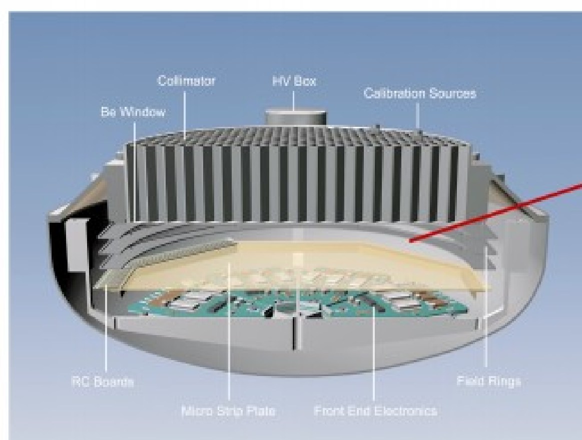

Cut-away drawing of the JEM-X detector (image: *JEM-X: The X-ray monitor aboard INTEGRAL*, N. Lund et al.)

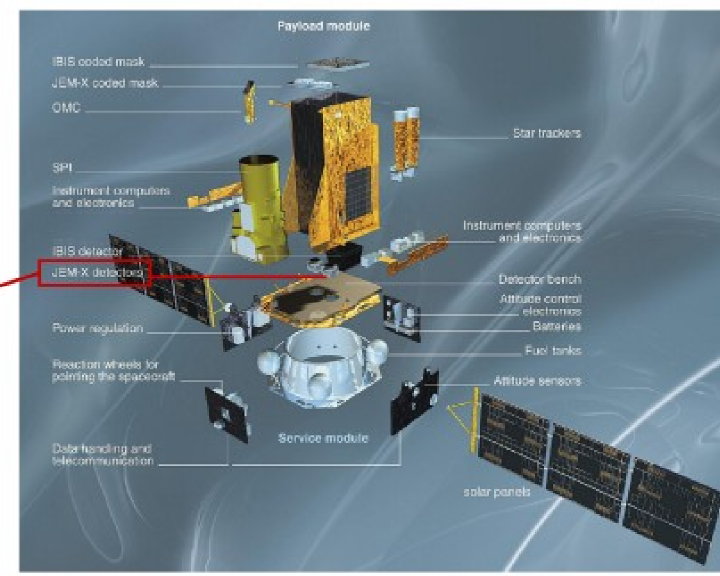

The INTEGRAL spacecraft (image credit: INTEGRAL consortium).

To improve: image of the miss science goal very general, time and angular resolution.

Points done well: CCD and MPE :)

eROSITA

CLEA SUNNY

ASTROCENT

eROSITA Detectors

- eROSITA (Extended Roentgen Survey with an Imaging Telescope Array) is the core instrument on the Spectrum-Roentgen-Gamma (SRG) mission.
- Its scientific goal is the exploration of the X-ray Universe in the energy band from about 0.3 keV upto 10 keV with excellent energy, time and spatial resolution and large effective telescope area.
- The eROSITA telescope consists of seven identical Wolter-1 mirror modules. Each module contains 54 nested mirror shells in order to meet the required sensitivity.
- A novel detector system has been developed by Max Planck Institute of Extraterrestrial Physics (MPE) on the basis of the successful XMM-Newton pnCCD technology.
- For the detection of the single X-ray photons with high resolution, adequate frame transfer pnCCDs and the associated front-end electronics have been developed.
- The back-illuminated, 450 μm thick and fully depleted pnCCDs with a 3 cm × 3 cm large image area have been produced in the course of further development of the XMM-Newton X-ray pnCCDs.

eROSITA Detectors

- The eROSITA chip is tailored to the requirement of the project such as the number of pixels, pixel size, the optional blocking filter, and a frame store section.
- All eROSITA pnCCDs were tested at chip-level including spectroscopic performance with a Fe-55 source by means of a unique so-called cold chuck probe station. Based on these results, seven best CCDs are selected for the eROSITA focal plane cameras.
- An analogue signal processor with 128 parallel channels has been developed for readout of the pnCCD signals. This ASIC permits fast and low-noise signal filtering.
- Even at the low X-ray energy of 280 eV, a spectrum of Gaussian shape with a FWHM of 52 eV is measured.
- A flight-like eROSITA camera has been assembled after successful development and the verification of the CCD and its signal processor chip.

To improve:

one full slide "lost" for science goal,

time resolution,

LOGOs important !

The Imaging X-ray Polarimetry Explorer

•Three identical grazing incidence telescopes (4 m focal length)

•X-ray-polarization-sensitive detector
- Gas Pixel Detector
- Position-dependent and energy-dependent polarization maps
- 12.9 arcmin square FOV
- Angular resolution ≤ 25 arcsec
- Energy resolution (FWHM) 0.57 keV @ 2 keV ($\propto \sqrt{E}$)
- Energy range 2-8 KeV

•Pointing mode

•X-ray polarimetry
•Polarimetric images
•Simultaneous spectral, spatial, and temporal measurements

• 9/12/2021 – 2024

Equatorial orbit at 600 km altitude

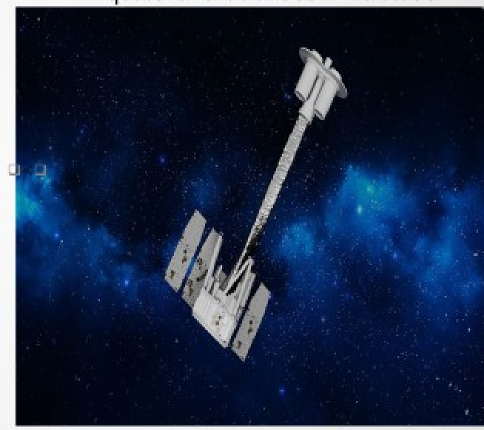

Objectives

- Emission mechanisms and geometry of AGNs
- Magnetars
- Pulsars
- How particles are accelerated in pulsar wind nebula

To improve: all resolutions, looks like slide from net.

CALET in a nutshell

- Mission has started in 2015 and it is still ongoing.
- It is part of the International Space Station.
- With an energy range between 7 keV and 1 TeV is aimed to study high-energy photons and cosmic ray particle detection.

Soft Gamma-ray Monitor (SGM)

- Bismuth germanate scintillation detector sensitive at energies from 100 keV to 20 MeV
- 102 mm diameter → 8 sr field of view

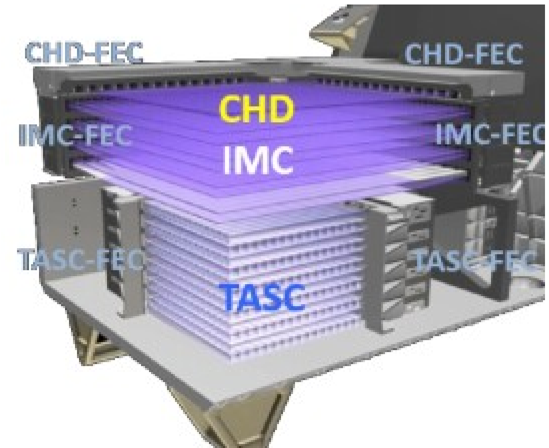

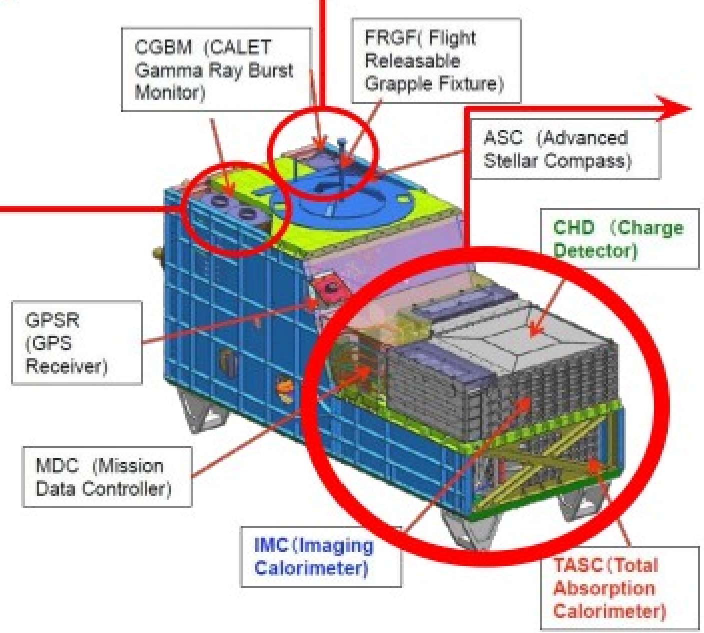

Hard X-ray Monitor (HXR)

- Two identical units of lanthanum bromide scintillation detector sensitive at energies from 7 to 1000 keV
- 61 mm diameter → 3 sr field of view

The CALET Calorimeter (CCAL)

Measures the cosmic-ray total electron spectrum from 1 GEV up to the TeV region. Build of:

- Charge Detector (CHD) – plastic scintillator hodoscope for absolute charge measurement (between 1 and ~40 Z)
- IMaging Calorimeter (IMC) – sampling calorimeter
- Total AbSorption Calorimeter (TASC) – lead tungstate hodoscope.

To improve:
time resolution,
angular resolution,
looks like slide
from net.

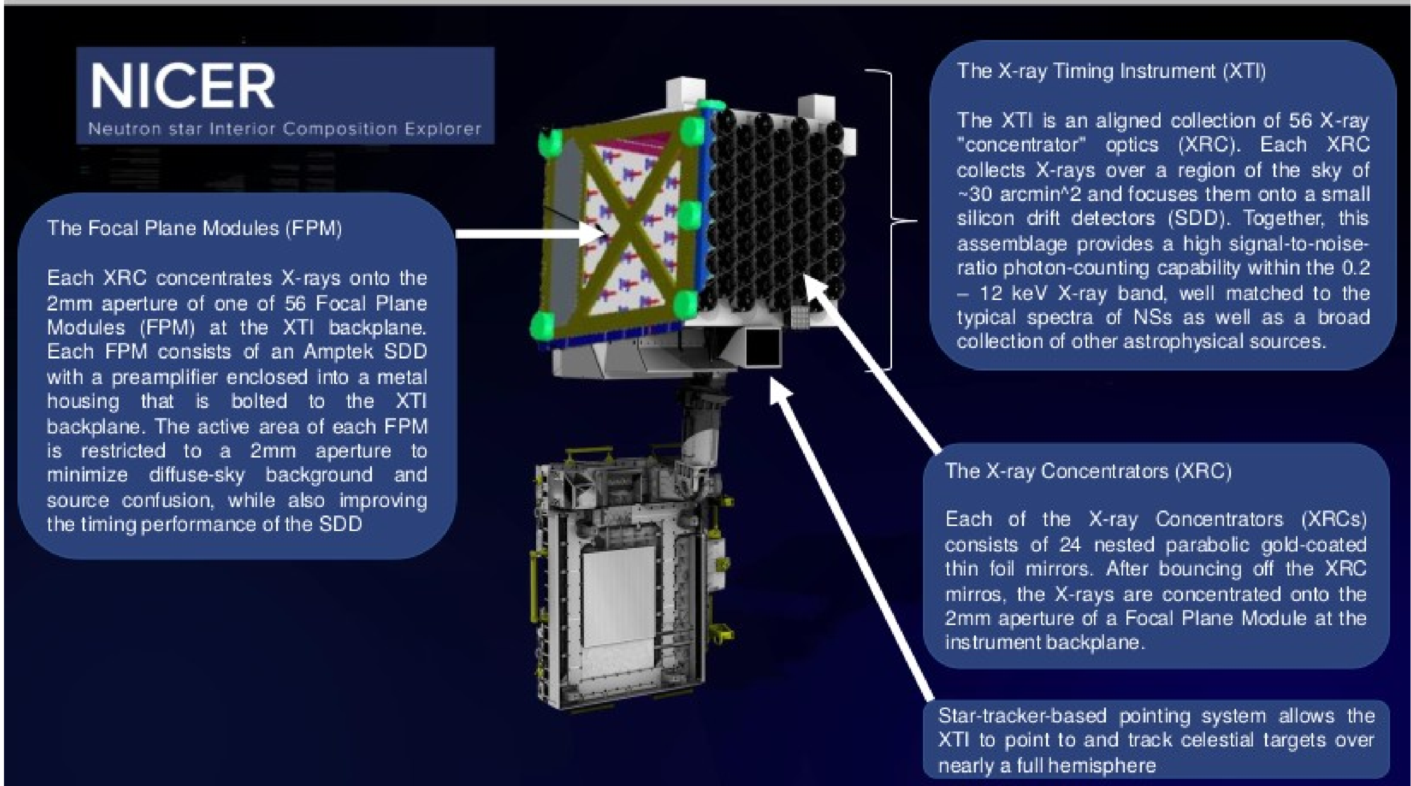

To improve:
time resolution,
angular resolution,
indicate the position

Chandra LETG

LETG - the Low Energy Transmission Grating provides:

- the highest spectral resolving power (E/ΔE > 1000) on Chandra at low energies: 0.07-0.15 keV
- moderate resolving power (E/ΔE ~ 20xλ) at higher energies: 0.25-4.13 keV

Scientific Objectives

The LETG is most commonly used for studies of bright point sources. The prime candidates for study in the Galaxy are **stellar coronae, white dwarf atmospheres, X-ray binaries,** and **cataclysmic variables**. Extragalactic sources include relatively bright **active galactic nuclei** and cooling flows in **clusters of galaxies**.

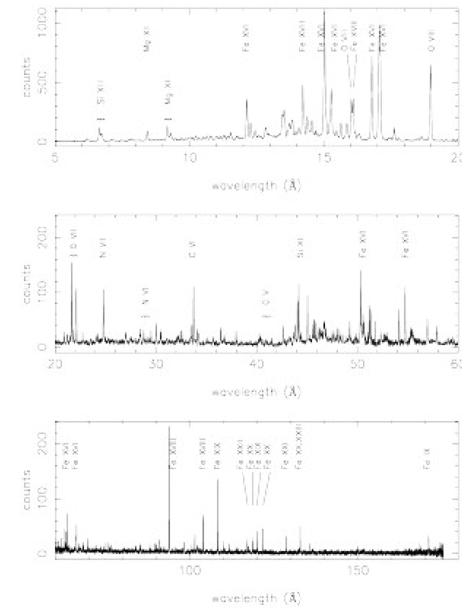

Fig. Extracted LETGS spectrum of Capella (Brinkman et al. 2000, ApJ, 530, L111).

Source: https://cxc.harvard.edu/cal/Letg/; https://cxc.harvard.edu/proposer/POG/html/chap9.html

Chandra LETG

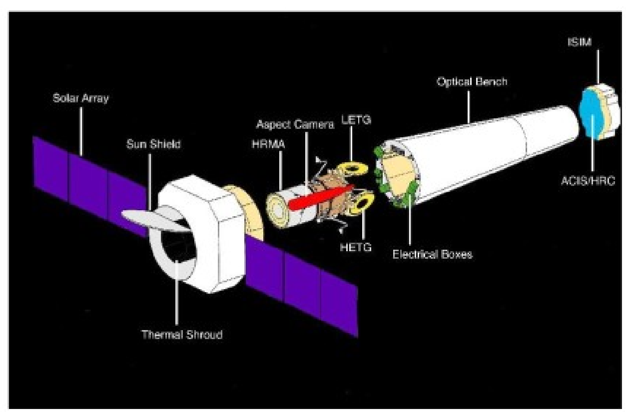

Instruments of LETG:

The primary detector designed for use with the Chandra LETG is High Resolution Camera spectroscopic array **HRC-S**.

The spectroscopic array of the Chandra CCD Imaging Spectrometer **ACIS-S** can be used as well, though with lower quantum efficiency below ~0.6 keV and a smaller detectable wavelength range.

- **LETG/HRC-S** wavelength range: 1.2- 175 Å, energy range: 0.070-10.0 keV
- **LETG/ACIS-S** wavelength range: 1.2-60 Å, energy range: 0.2-10.0 keV

Source: https://cxc.harvard.edu/cal/Letg/; https://cxc.harvard.edu/proposer/POG/html/chap9.html and https://cxc.harvard.edu/ciao/workshop/oct08/talks/huenemoerder.pdf

To improve:
energy resolution – hard for energetic photons, indicate the position of the detector.

FERMI Gamma-Ray Telescope Gamma-ray Burst Monitor (GBM)

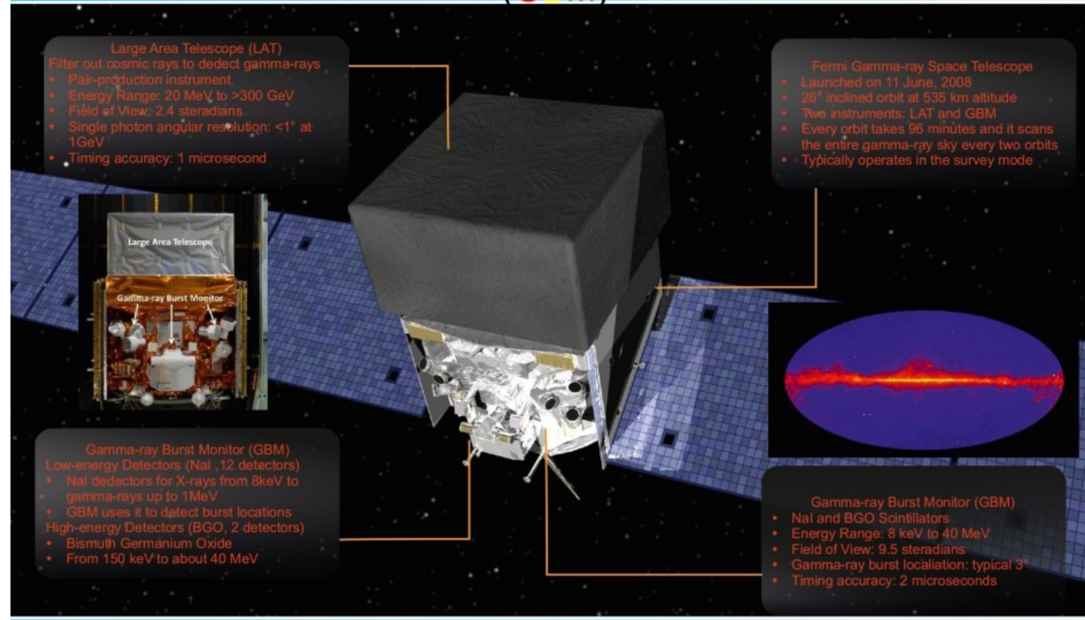

Science Cases

- Gamma-ray Burst Events
- Solar Flares
- Gamma-ray Millisecond Pulsars (The first observation)
- Novae
- Synergy with LIGO and VIRGO for Gws
- Active Galaxies
- Supernova Remnants (SNRs)
- Cosmic-ray Sources (e.g. shock waves in a SNR)
- Galactic Center
- Fermi Bubbles

To improve:
energy resolution,
taken from net,
already summary,
Nutshell is a plan for
future mission.

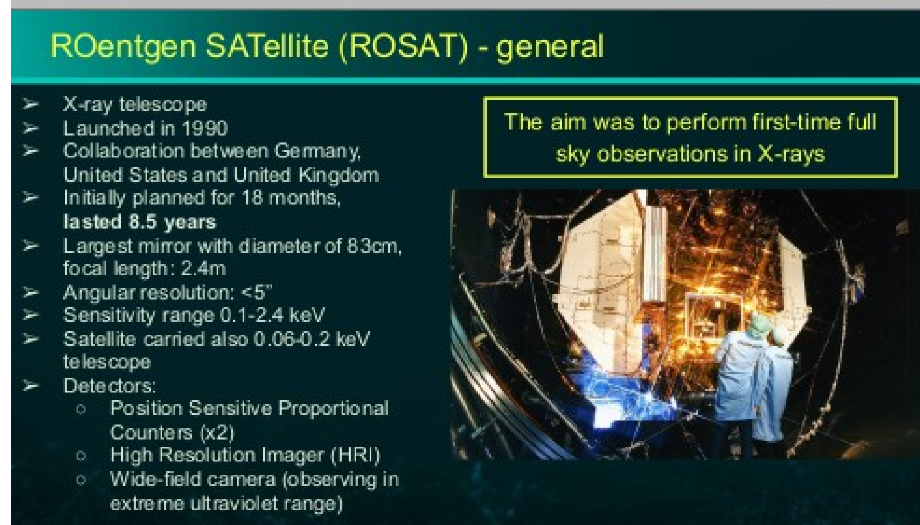

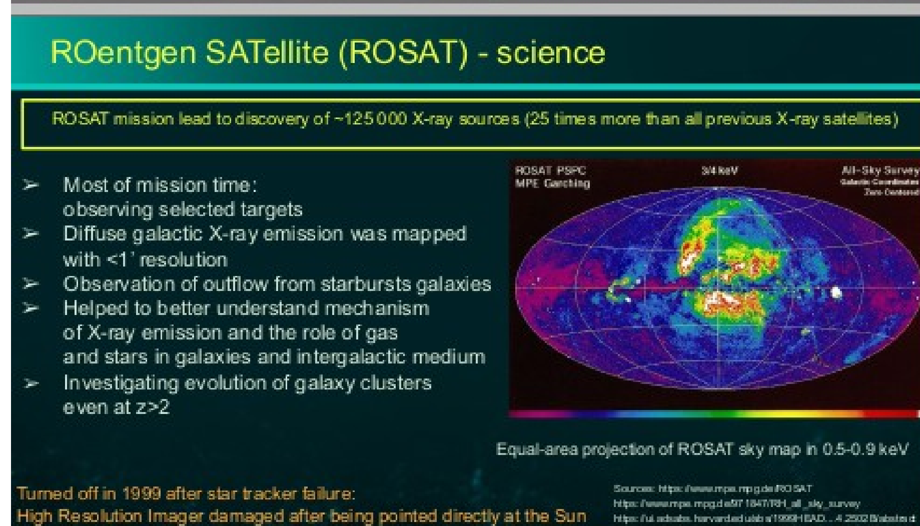

To improve: all resolutions, looks like slide from net, science goals?

Suzaku XIS (X-Ray Imaging Spectrometer)

- Instrument launched on Suzaku X-ray astronomy satllite (Astro-E2) (Fig. 1) developed jointly by JAXA and NASA and launched on 10.07.2005.
- Suzaku XIS weight 48.7kg, power consumption 67 W, bus voltage 50 V.
- Instrument is combined of four Si-based X-ray charge coupled device (CCD) cameras (one sensor on Fig. 2).
- In the x-ray sensor photons are converted to electricity via photoelectric absorption, the energy of photon is measured as amount of charge produced.
- Each XIS have its own, independent X-Ray telescope (XRT) (Fig. 3), mirror diameter 399mm, focal length 4.75m, weight 19.5kg. This gives four XRT in total used by XIS, layout of telescopes on Suzaku satellite could be found on (Fig. 4), XRT-I0, XRT-I1, XRT-I2, and XRT-I3 are telescopes for XIS instrument. Imaging area is exposed to the sky for observations, while frame storage area is shielded.
- Each CCD camera has single CCD chip with 1024px x 1024px resolution (Fig. 5), and capability to cover 18 arc' x 18 arc' of its frontal view.
- XIS operates in photon-counting mode, and each incoming photon energy, position and event time are reconstructed.
- Energy band of XIS instrument is in 0.2 – 12.0 keV range.
- XIS1 is back illuminated (BI) while XIS0, XIS2, and XIS3 are front illuminated (FI) chips (Fig. 6). Each chip is divided into four segments (A, B, C, D), to make readout more efficient (each segment has separate redout node (Fig. 5)).
- For calibration purpose each XIS unit was equppied with three ^{55}Fe, with half life of 2.73 yr. Sources emits strong lines at 5.9 keV and 6.5 keV.

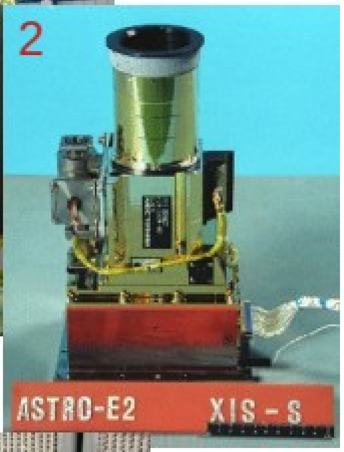

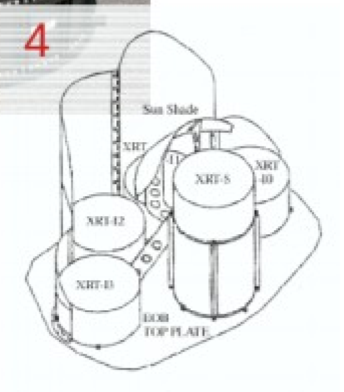

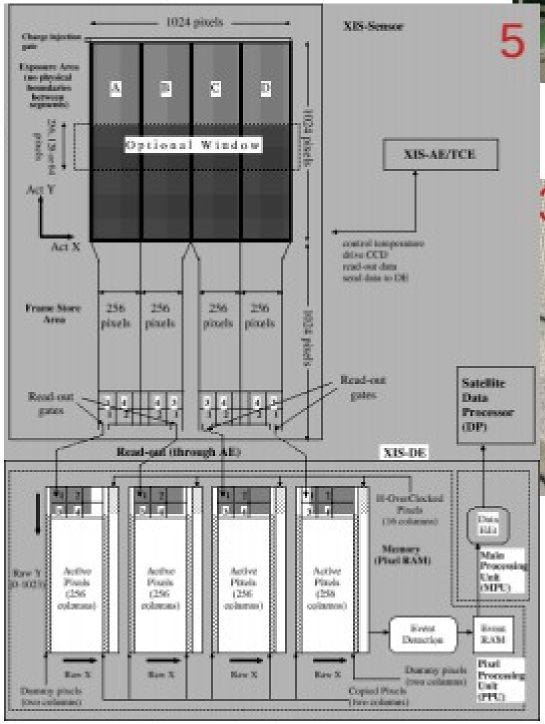

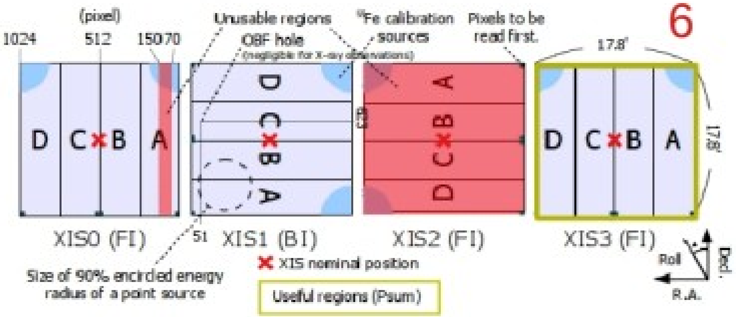

Libs:

- http://www.astro.isas.jaxa.jp/suzaku/doc/suzaku_td/node10.html
- http://www.astro.isas.jaxa.jp/suzaku/doc/suzaku_td/node9.html
- https://heasarc.gsfc.nasa.gov/docs/suzaku/about/xis_inst.html
- https://heasarc.gsfc.nasa.gov/docs/suzaku/about/xrt_inst.html
- https://heasarc.gsfc.nasa.gov/docs/suzaku/analysis/abc/node9.html

To improve:
looks like slide
from net,
it is perfect,
only arrow
can be added.

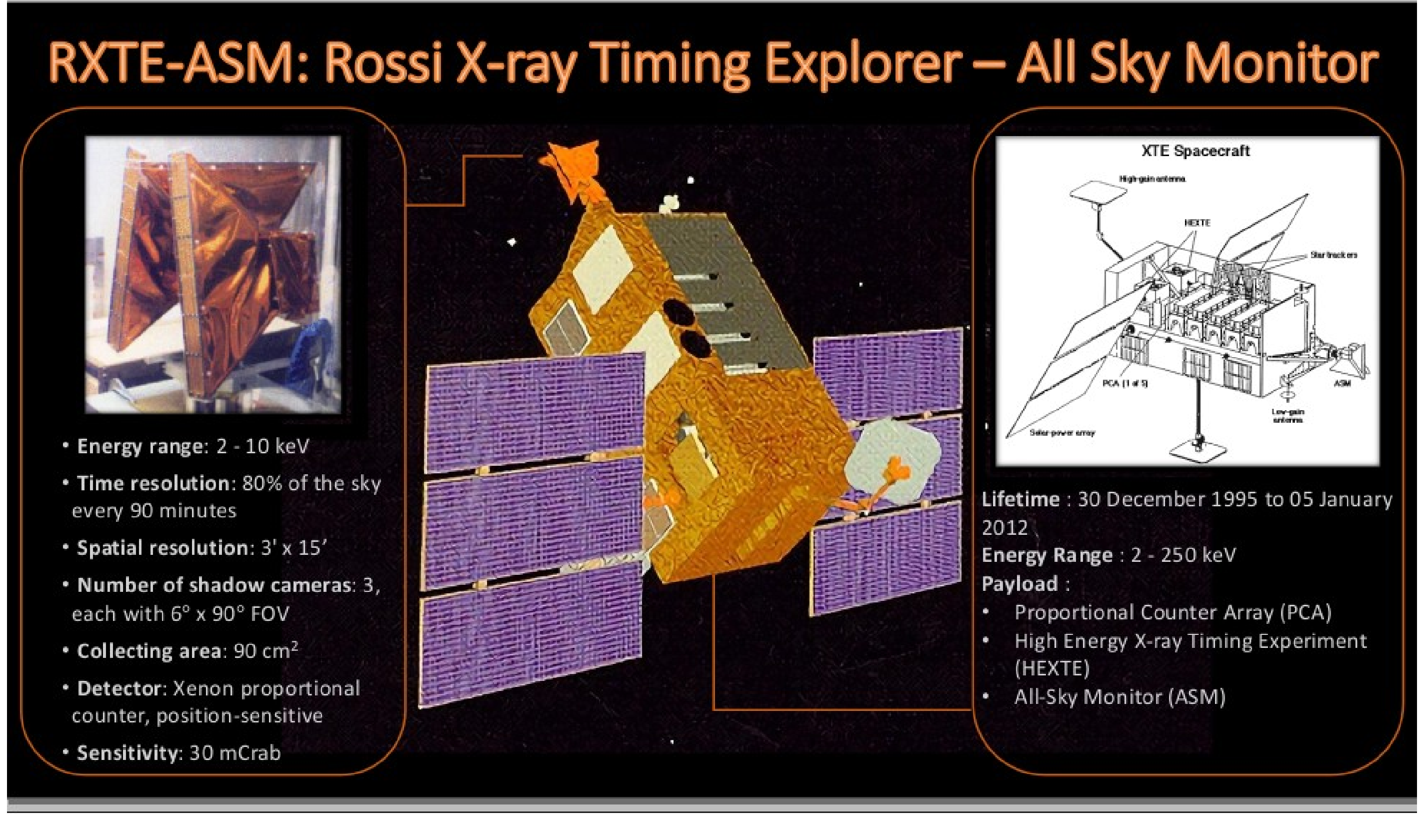

Science goals

- Very large collecting area and all-sky monitoring of bright sources
- Discovery of kilohertz QPO’s
- Discovery of spin periods in LMXRB
- Detection of X-ray afterglows from Gamma Ray Bursts
- Extensive observations of the soft state transition of Cyg X-1
- Observations of the Bursting Pulsar over a broad range of luminosities, providing stringent test of accretion theories.

To improve: where is HEXTE, angular and energy resolutions, HEXTE photo.

RXTE

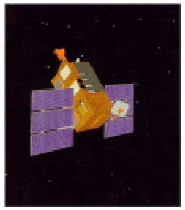

RXTE - Rossi X-ray Timing Explorer was a NASA X-ray telescope operating from December 1995 to January 2012.

RXTE was equipted with a All Sky Monitor (ASM) and 2 main instruments the Proportional Counter Array (PCA) and the High Energy X-ray Timing Experiment (HEXTE).

More details about HEXTE are given in the next slide.

RXTE HEXTE

- Energy rate: 15-250 keV.
- Time sampling: 8 microseconds
- Field of view: 1° FWHM
- Detectors: 8 sodium-iodide crystal that are gathered into two clusters, each containing 4 detectors.
- Sensitivity: 360 count/second per HEXTE cluster (1 Crab Nebula intensity).
- Background: 50 count/second per HEXTE cluster

To improve:

completed, maybe from net, but has everything what is important, angular resolution.

RXTE PCA: Rossi X-ray Timing Experiment Proportional Counter Array

Launched 30 December 1995

3 different instruments

One of the instruments: PCE

5 proportional counters

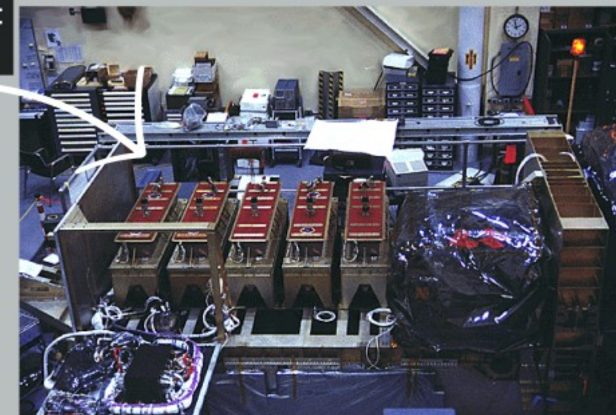

Properties

- Energy range: 2 - 60 keV
- Energy resolution: <18% at 6 keV
- Time resolution: 1 microsec
- Collecting area: 6500 cm^2
- Sensitivity: 0.1 mCrab
- Background: 90 mCrab

Mission

- Study galactic and extragalactic X-ray sources
- Detect faint transients in regions where the All-sky monitor is not reliable
- Result: discovered many new millisecond X-ray pulsars

To improve:

time resolution,
two detectors,
the second
XTEND or XTREND?
should have at least
angular resolution,
since it is imager.

X-Ray Imaging and Spectroscopy Mission (XRISM)

Sudhagar Suyamprakasam : CAMK - PAN

Objective:

To investigate celestial X-ray objects in the Universe with high-throughput imaging and high-resolution spectroscopy.

X-ray telescope info:

- XRISM Formerly known as XARM.
- Collaboration & Participaion: JAXA, NASA & ESA.
- Mission instruments:
  - Resolve: Soft X-ray micro calorimeter
  - Xtend: Wide-field soft X-ray imager
- Design life: 3 years
- Number of mirror assemblies: 2
  - Over 3200 individual mirror segments.
  - Each mirror assembly is about 45 cm.
  - Resolution of just over 1'
- Launch Details:
  - Expected launch: 2023
  - Launch vehicle: JAXA HII-A rocket
  - Launch place: Japan's Tanegashima Space Center.

XRISM.
Credit: JAXA/NEC

Resolve Specifications:

XRISM Calorimeter
Credit: Larry Gilbert/NASA

- Micro Calorimeter Array: 6 x 6 pixel
- Each pixel size: 30''
- Energy Resolution: 5-7 eV
- Energy Band: 0.3 to 12 keV
- Field of View: 3' x 3'
- Angular Resolution: 1.7' (HPD)

Xtrend Specifications:

- Number of CCD Array: 4
- Energy Band: 0.4 to 13 keV
- Field of View: 38' x 38'

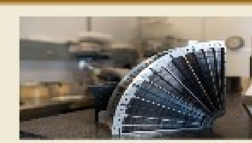

One qudrant of X-ray mirror
Credit: Taylor Mickal/NASA

Scientific goal categories:

- Structure formation of the Universe and evolution of clusters of galaxies.
- Circulation history of baryonic matter in the Universe.
- Transport and circulation of energy in the Universe.
- New science with unprecedented high-resolution X-ray spectroscopy.

Click Reference for further details: [1] NASA-HEASARC, [2] NASA-XRISM-science-instruments, [3] ArXiv:2003.04962

To improve:

PSF gives angular resolution - OK,

energy resolution.

Second slide is not needed.

Swift X-Ray Telescope

The XRT acquires images and obtain spectra of GRB afterglows.

Its primary function is to provide a accurate position (5 arcsec) to the BAT.

It sends this position to Gamma-ray Co-ordinate Network for ground-based follow-up observations.

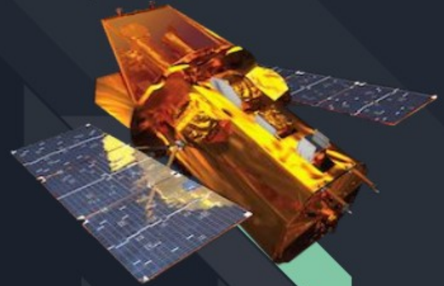

Telescope Description:

Telescope	JET-X Wolter I
Focal Length	3.5 m
Effective Area	110 cm^2@ 1.5 keV
Telescope PSF	18 arcsec HPD @ 1.5 keV
Detector	EEV CCD-22, 600 x 600 pixels
Detector Operation	Imaging, Timing, and Photon-counting
Detection Element	40 x 40 micron pixels
Pixel Scale	2.36 arcsec/pixel
Energy Range	0.2-10 keV
Sensitivity	8×10^{-14} erg $cm^{-2}s^{-1}$ in 10^4 seconds

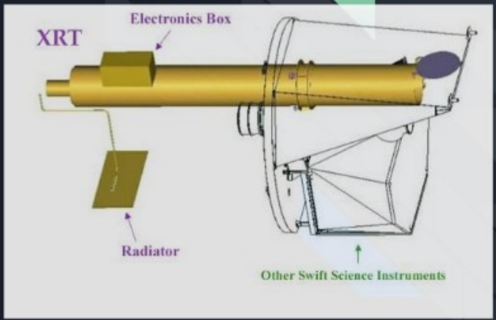

Modes of XRT:

a. **Image Mode:**
XRT has two integration times in imaging modes (depending on brightness of the target):
I. 0.1 second exposure
II. 2.5 second exposure

b. **Photodiode Mode:**
It is the highest timing resolution (10 μs) to detect rapid changes in the light-curve and high-resolution spectroscopy.

c. **Photon-Counting Mode:**
It provides 2-dimensional imaging, high spectral resolution and low timing resolution (2.5 s) for fluxes.

d. **Telescope Alignment Correction:**
To get the pointing accuracy of 5 arcsec Star Trackers are mounted on the forward telescope tube.
Telescope Alignment Monitor Assembly measures of the movement of XRT.

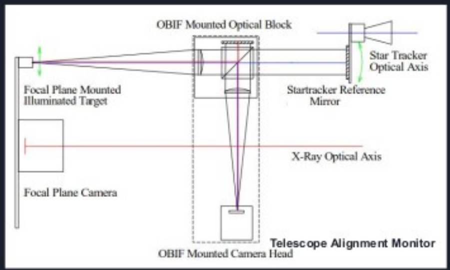

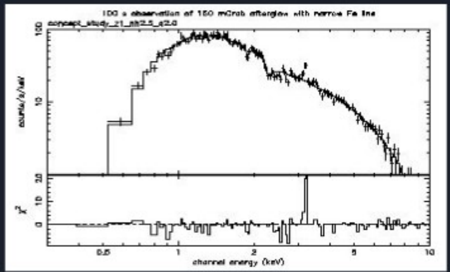

References:
1. https://swift.gsfc.nasa.gov/about_swift/xrt_desc.html
2. https://imagine.gsfc.nasa.gov/observatories/learning/swift/multimedia/spacecraft_art_gallery.html
3. DOI = 10.1117/12.618026

To improve:

nice and completec
all resolutions are
listed,

all images are
presented.

Nuclear Spectroscopic Telescope Array (Harrison et al. 2013)

Presentation: Tathagata Saha

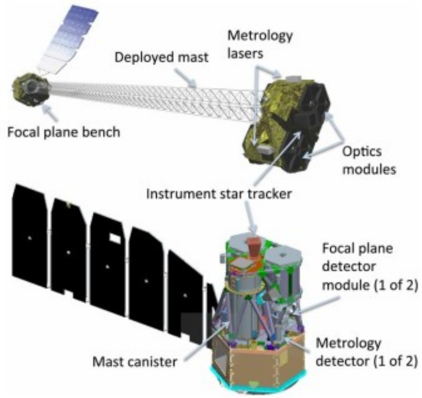

Optics:
- Wolter-1 configuration
- Optics arranged on the top the mast
- Focal length ~ 10m
- 133 shells

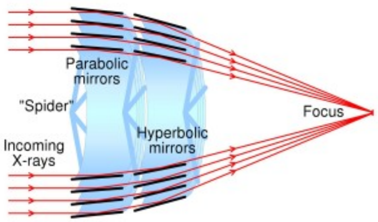

Wikimedia commons

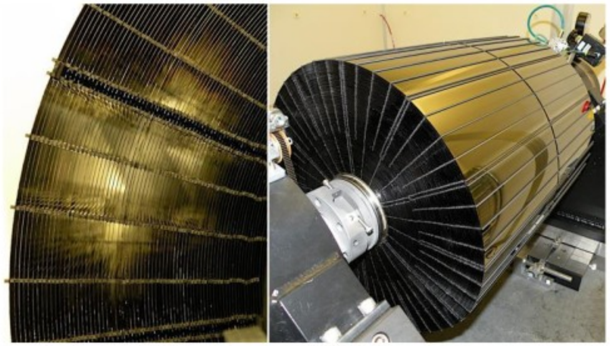

NASA/JPL

DETECTOR: The Focal Plane Modules (FPM)- Harrison et al. 2013

- CZT detectors: CdZnTe high cross section at 10-100 keV (than Si) and **higher quantum efficiency**.
- 2 FPM detectors
- Spatial resolution: 18" (Chandra - 0.5" for comparison)
- Energy resolution: 0.4 keV at 6 keV, 0.9 keV at 60 keV (FWHM)
- Time resolution ($\sigma_{t,event}$) = 2 microseconds accuracy for registering event time.
- Energy range: ~3-78 keV
- Science Goals:
  - Accretion physics : ULXs and Black hole binaries
  - Accretion physics AGNs: Compton Reflection and C-thick AGNs
  - Magnetars
  - Galaxy clusters
  - Solar physics

HIGHER EFFECTIVE AREA IN HARDER X-RAYS

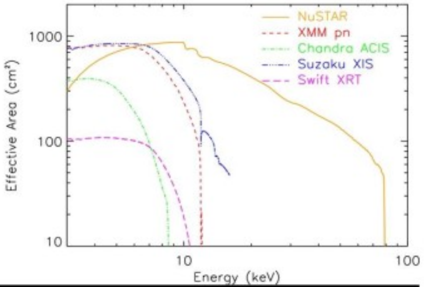

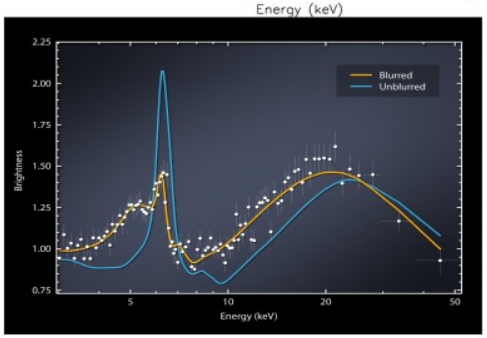

Compton Reflection: Caltech/NASA JPL

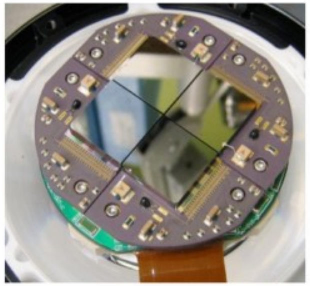

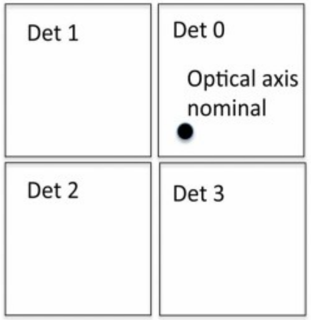

One of the detector modules

To improve:

nice and completed, but what and where is SPI?

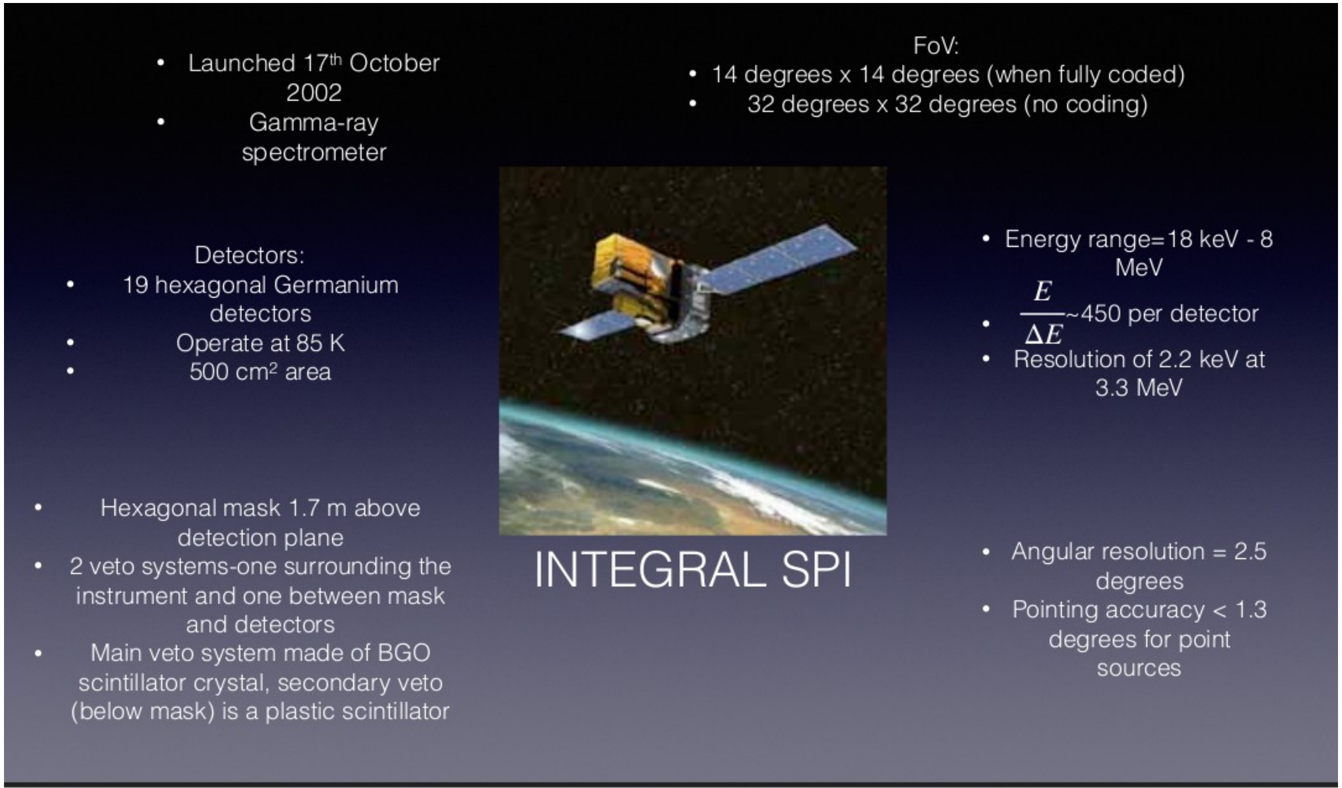

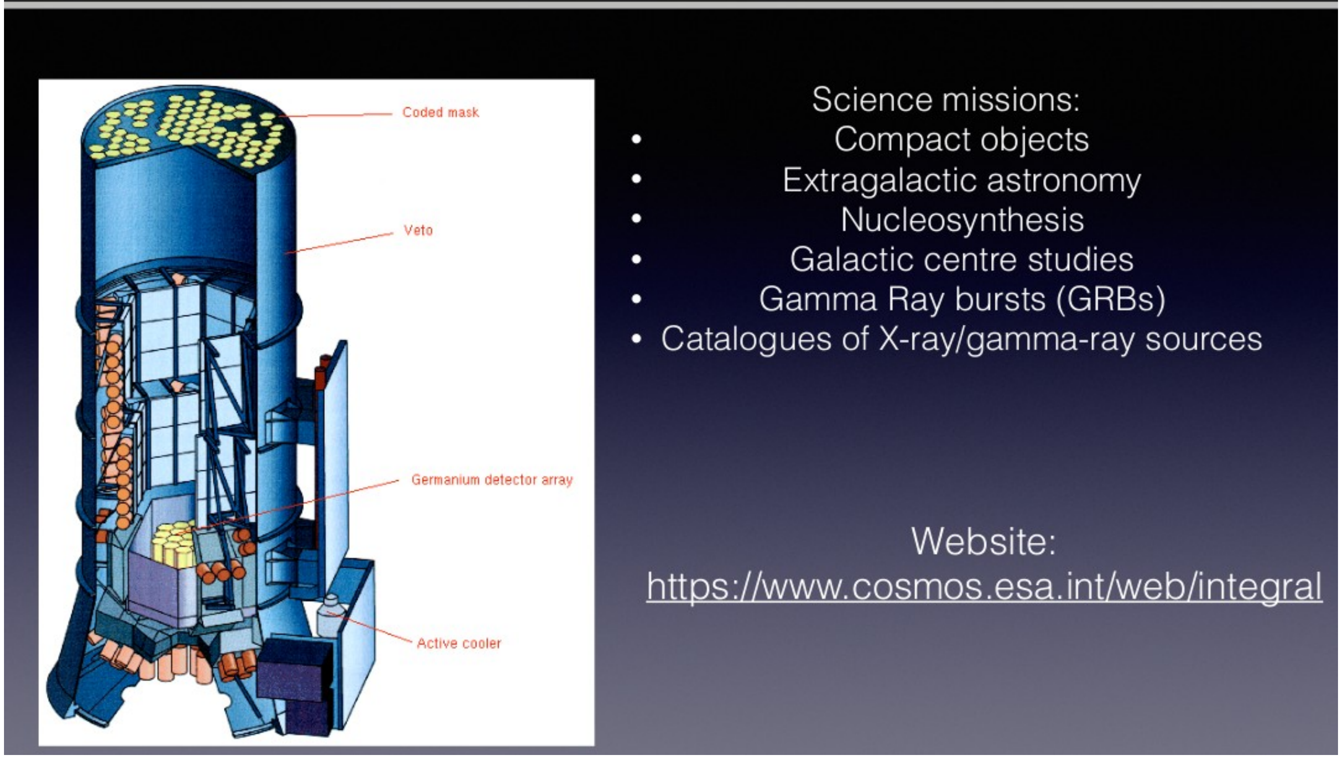

To improve:

some text is not visible,
where in the contex
of the whole
mission?

Chandra High Energy Transmission Grating (HETG)

- HETG is placed behind the Chandra mirrors.
- HETG consists of 336 gold grating facets as shown in the figure.
- The HETG gratings are designed to cover an energy range of 0.4 to 10 keV.
- The inner two rings are high-energy grating, HEG, facets, and the outer two rings are medium-energy grating, MEG, facets.
- The HETG intercepts the X-rays reflected from the mirrors, changing their direction by amounts that depend sensitively on the X-ray energy.
- One of the focal plane detectors records the location of the diffracted X-rays, enabling a precise determination of their energies.
- The HETG has been used to measure Doppler velocities of orbiting systems, even as low as 50 km/s, and plasma outflow velocities from a few hundred to 10's of thousands of km/s.

Image credit:https://space.mit.edu/HETG/HETG_8bit.gif

HETGS Range:	0.4–10.0 keV, 31–1.2Å
HEG Range:	0.8–10.0 keV, 15–1.2 Å
MEG Range:	0.4–5.0 keV, 31–2.5 Å
Effective Area (see Figures 8.7 8.8):	7 cm^2 @ 0.5 keV
(MEG+HEG first orders,	59 cm^2 @ 1.0 keV
with ACIS-S)	200 cm^2 @ 1.5 keV
	28 cm^2 @ 6.5 keV
Resolving Power (E/ΔE, λ/Δλ)	
HEG:	1070–65 (1000 @ 1 keV, 12.4 Å)
MEG:	970–80 (660 @ 0.826 keV, 15 Å)
Resolution:	
ΔE:	0.4–77 eV FWHM
Δλ, HEG:	0.012 Å FWHM
Δλ, MEG:	0.023 Å FWHM
Absolute Wavelength Accuracy: (w.r.t. "theory")	
HEG	±0.006 Å
MEG	±0.011 Å
Relative Wavelength Accuracy: (within and between obs.)	
HEG	±0.0010 Å
MEG	±0.0020 Å
HEG angle on ACIS-S:	−5.235° ±0.01°
MEG angle on ACIS-S:	4.725° ±0.01°
HETGS Rowland spacing	8632.65 mm (flight installed)
Wavelength Scale:	
HEG	0.0055595 Å / ACIS pixel
MEG	0.0111200 Å / ACIS pixel
HETG Properties:	
Diffraction Efficiency:	2.5% @ 0.5 keV (MEG)
(single-side, first order)	19% @ 1.5 keV (MEG & HEG)
	9% @ 6.5 keV (HEG)
HETG Zeroth-order Efficiency:	4.5% @ 0.5 keV
	8% @ 1.5 keV
	60% @ 6.5 keV
Grating Facet Average Parameters	
HEG and MEG bar material:	Gold
HEG / MEG period:	2000.81 Å , / 4001.95 Å
HEG / MEG Bar thickness:	5100 Å , / 3600 Å
HEG / MEG Bar width:	1200 Å , / 2080 Å
HEG / MEG support:	9800 Å, / 5500 Å polyimide

Table: HETG Parameters
Credit: https://cxc.harvard.edu/cal/Hetg/

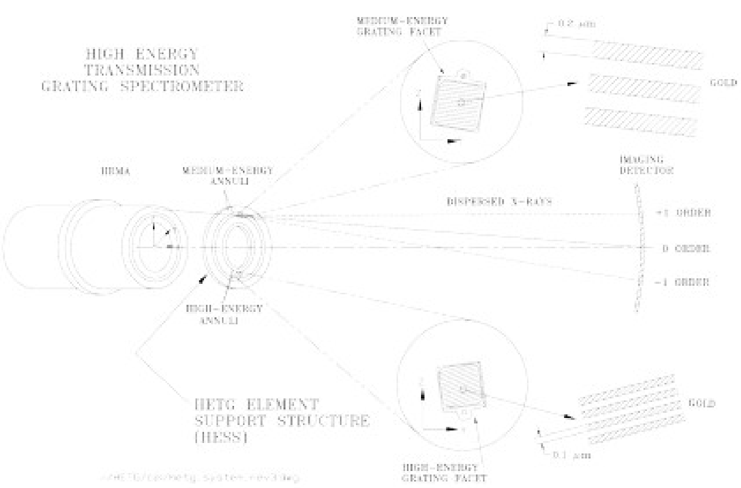

A schematic layout of the High Energy Transmission Grating Spectrometer.(The HETG provides spectral separation through diffraction.)

(Image credit: https://cxc.harvard.edu/proposer/POG/html/images/hetgslayout.png)

To improve: two slides less, numbers needed, observational results instead of observational goals.

XMM-NEWTON

Iftikhar Ahmad

3rd year Ph.D. student

European Union ASTROCENT

XMM-NEWTON

- The Multi-Mirror Mission (XMM-Newton) was launched in 1999.
- The large collecting area and ability to make long uninterrupted exposures provide highly sensitive observations.
- Since Earth's atmosphere blocks out all X-rays, only a telescope in space can detect and study celestial X-ray sources.
- The XMM-Newton mission is helping scientists to solve a number of cosmic mysteries, ranging from the enigmatic black holes to the origins of the Universe itself.

Characteristics of XMM-Newton

- Simultaneous operation of all scientific instruments
- High sensitivity
- Good angular resolution
- High spectral resolution
- Simultaneous optical/UV observations
- Long, continuous visibility of the target

Objectives

- Investigate spectra of cosmic X-ray sources
- Perform sensitive medium-resolution spectroscopy
- Broad band imaging spectroscopy from 150 eV to 15 keV
- Simultaneous sensitive coverage of the wavelength band 1700 to 6500 Å

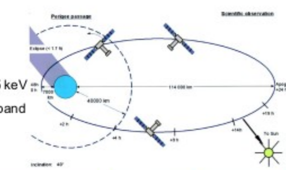

Scientific Instruments

- European Photon Imaging Camera (EPIC)
- Reflection Grating Spectrometer (RGS)
- Optical Monitor (OM)

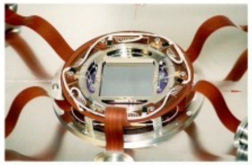

EPIC

- EPIC cameras offer the possibility to perform extremely sensitive imaging observations over the telescope's field of view (FOV) of 30 arcmin.
- EPIC focal plane imaging spectrometers on XMM-Newton uses CCDs to record the images and spectra of celestial X-ray sources focused by the three X-ray mirrors.
- EPIC observes in the 0.2-12 keV band and consists of two MOS and one PN CCD arrays.

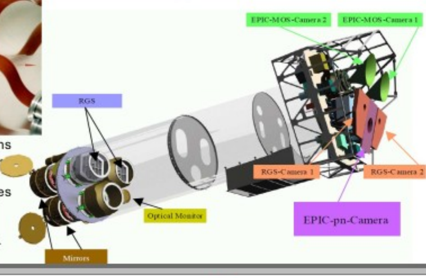

European Union ASTROCENT

Combining the images from all EPIC cameras, the Lockman Hole provides the deepest ever X-ray survey of this region. The view gives a 'real colour' representation of all the sources, coded according to their X-ray hardness: red, green and blue correspond to the 0.5-2, 2-4.5 and 4.5-10 keV range, respectively. (see also: astro-ph/0310804).

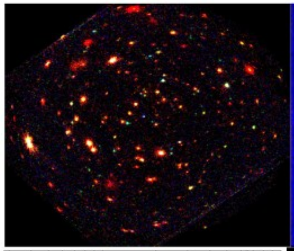

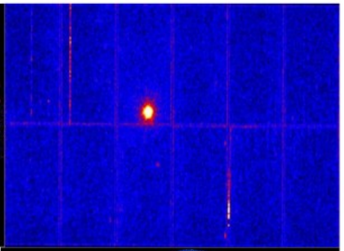

Composite image of Swift J1818.0–1607, the youngest pulsar (magnetar) ever observed, as seen by the EPIC-pn camera on ESA's XMM-Newton. The image combines observations in the following energy bands: 2–4 keV (red), 4–7.5 keV (green) and 8.5–12 keV (blue). See P. Esposito et al. (2020)

The line spectrum of the cluster 2A0335+096, as observed with XMM-Newton EPIC (from Werner et al. 2006b)

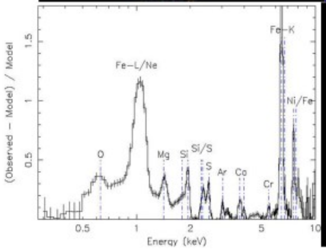

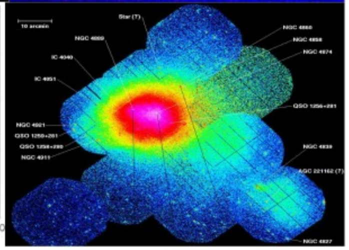

XMM-Newton has again observed the Coma Cluster of galaxies, with far longer exposures. Certain regions were observed for 22.6 Ksecs instead of 3.4 Ksecs originally, and with a lower proton background. EPIC-pn image covers the 0.3 to 2.0 keV energy range and clearly discerns far more sources. The difference is striking particularly in the north/west (upper-right) corner. credit: ESA/XMM-Newton

European Union ASTROCENT

Thank you

Part 2. **OBSERVATIONS**

Lecture 5: Statistics of measurements

Do we measure the source or simply fluctuation in the noise:

- instrumental noise, spurious signals in the absence of any photons, (CCDs, PC, readout processes):
  i) *statistical* in nature – i.e. due to randomly arriving cosmic rays
  ii) *systematical* in nature – i.e. aging of detector

- statistical fluctuations - "noise" inherent randomness of certain types of events.

We measure the rate of arrival of photons in a limited time interval.

Poisson distribution:

Consider source of constant luminosity (not pulsating), that produces, on average, 100 counts every second. 10 ms between each count.

Poisson distribution:

Consider source of constant luminosity (not pulsating), that produces, on average, 100 counts every second. 10 ms between each count.

Each photon arrives at a time completely uncorrelated with each others (randomly)

Poisson distribution:

Consider source of constant luminosity (not pulsating), that produces, on average, 100 counts every second. 10 ms between each count.

Each photon arrives at a time completely uncorrelated with each others (randomly).

Average time of arrival is governed by fixed *probability* of an event occurring in some fixed interval of time.

Poisson distribution:

Consider source of constant luminosity (not pulsating), that produces, on average, 100 counts every second. 10 ms between each count.

Each photon arrives at a time completely uncorrelated with each others (randomly).

Average time of arrival is governed by fixed *probability* of an event occurring in some fixed interval of time.

A distribution of counts $N(x)$ can be obtained from many measurements: $N(105)$, $N(95)$, $N(87)$, $N(101)$ ... in 1 s intervals.
N – number of times
x – a given value occurs.

Poisson distribution:

For a random process such as photon arrival time, this distribution is well known theoretically as Poisson distribution:

$$P_x = \frac{m^x e^{-m}}{x!}$$

Poisson distribution:

For a random process such as photon arrival time, this distribution is well known theoretically as Poisson distribution:

$$P_x = \frac{m^x e^{-m}}{x!}$$

m – average (mean) number of events over a large number of tries,

x – integer number of events (counts).

if m=10.3 P(6 photons) = 0.056

if m=6 P(6 photons) = 0.161 but < 1

It is not particularly likely that one will detect the mean number.

Poisson distribution:

Is valid for discrete independent events that occur randomly (equal probability of occurrence per unit time) with a low probability of occurrence in a differential time integral *dt*.

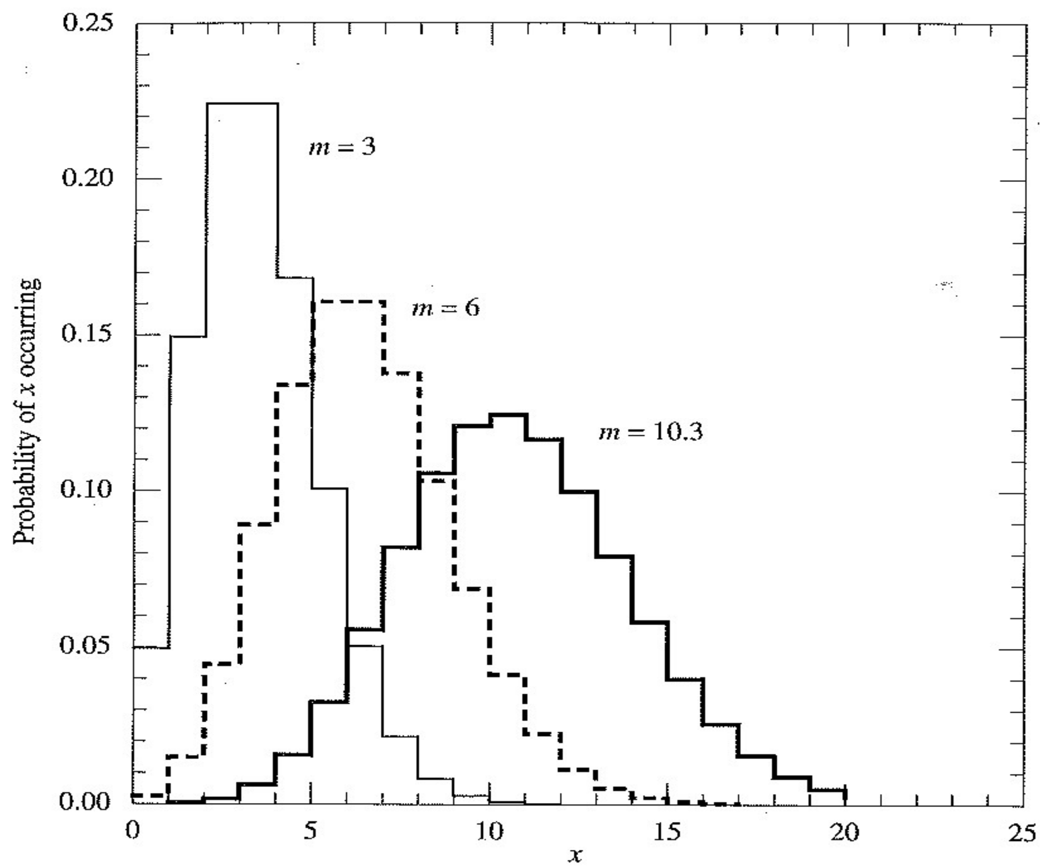

Figure 6.7. The Poisson distribution for small mean numbers, $m = 3.0$, 6.0 and 10.3. The ordinate gives the probability of the value x occurring, for the given mean value. Note the asymmetry of the histograms.

Poisson distribution:

$$\sum_{x=0}^{x=\infty} P_x = 1$$

- *distribution i.s not symmetric,*
- *more symmetric for higher m.*

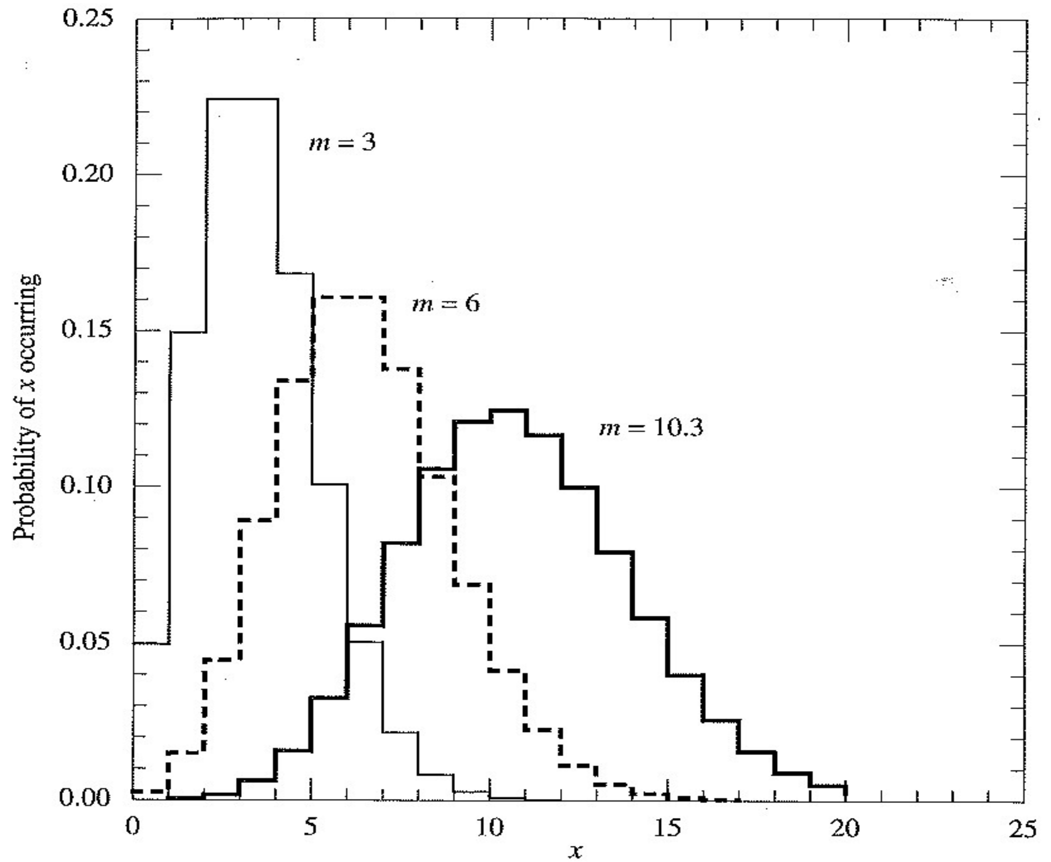

Figure 6.7. The Poisson distribution for small mean numbers, $m = 3.0$, 6.0 and 10.3. The ordinate gives the probability of the value x occurring, for the given mean value. Note the asymmetry of the histograms.

Poisson distribution:

-probability of obtaining non zero event is significant.

Table 6.1. *Sample values of Poisson function P_x*

x:	0	1	2	3	4	5	6	7^a	8	9
$m = 1$	0.368	0.368	0.184	0.061	0.015	0.003	0.001	7E–5	9E–6	1E–6
$m = 2$	0.135	0.271	0.271	0.180	0.090	0.036	0.012	0.003	0.001	2E–4
$m = 3$	0.050	0.149	0.224	0.224	0.168	0.101	0.050	0.022	0.008	0.003
$m = 4^b$	0.018	0.073	0.147	0.195	0.195	0.156	0.104	0.060	0.030	0.013
$m = 6^c$	0.002	0.015	0.045	0.089	0.134	0.161	0.161	0.138	0.103	0.069
$m = 10^d$	5E–5	5E–4	0.002	0.008	0.019	0.038	0.063	0.090	0.113	0.125

[a] The notation 7E-5 indicates 7×10^{-5}.
[b] The values of P_x for $m = 4$ at $x = 10$ and 11 are 0.005 and 0.002 respectively.
[c] The values of P_x for $m = 6$ at $x = 10–14$ are 0.041, 0.023, 0.011, 0.005, 0.002.
[d] The values of P_x for $m = 10$ at $x = 10–18$ are: 0.125, 0.114, 0.095, 0.073, 0.052, 0.035, 0.022, 0.013, 0.007.

Normal distribution, Gaussian:

Continuous and symmetrical distribution which gives the *differential probability dP* of finding the value x within the differential interval *dx*:

$$dP_x = \frac{1}{\sigma_w \sqrt{2\pi}} \exp\left[\frac{-(x-m)^2}{2\sigma_w^2}\right] dx$$

Normal distribution, Gaussian:

Continuous and symmetrical distribution which gives the *differential probability dP* of finding the value x within the differential interval *dx*:

$$dP_x = \frac{1}{\sigma_w \sqrt{2\pi}} \exp\left[\frac{-(x-m)^2}{2\sigma_w^2}\right] dx$$

m – the mean, which is the true value of the quantity being measured,

σ_w - width, the standard deviation of the distribution.

Two parameters instead of one in Poisson distribution.

Normal distribution, Gaussian:

Bell curve of probability, symmetric around *m*, can extend to negative values of *x*.

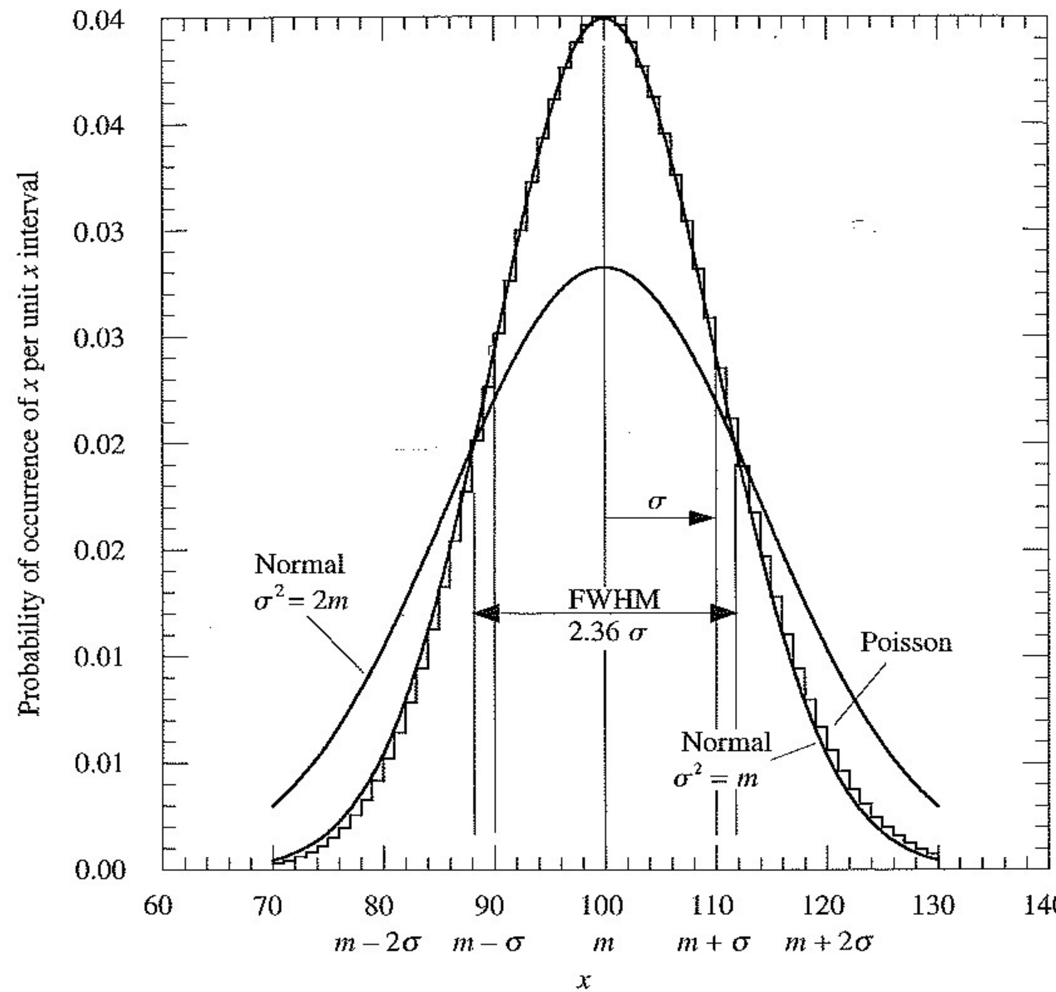

Figure 6.8. The Poisson (step curve) and normal distributions (smooth curves) for the mean value $m = 100$. The normal distribution is given for two values of the width parameter σ_w which is shown in the text to be equal to the standard deviation σ. The Poisson distribution approximates well the normal distribution if the latter has $\sigma = \sqrt{m}$. Note the slight asymmetry of the Poisson distribution relative to the normal distribution. The standard deviation and full width half maximum widths are shown for the higher normal peak; the two normal curves happen to cross at the FWHM point.

Normal distribution, Gaussian:

Bell curve of probability, symmetric around *m*, can extend to negative values of *x*.

$$(2\pi)^{-1/2}$$

is chosen so that this distribution is also normalized:

$$\int_{x=-\infty}^{x=\infty} dP_x = 1$$

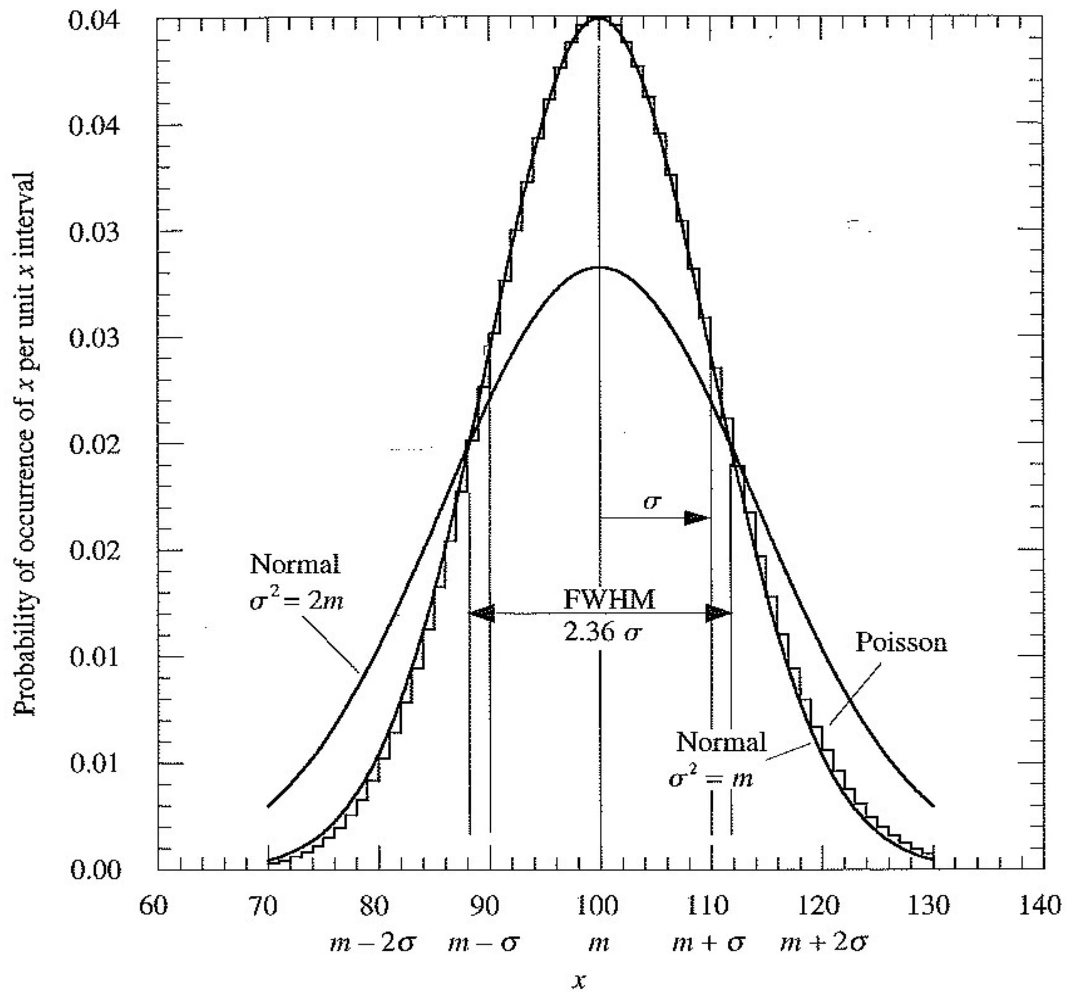

Figure 6.8. The Poisson (step curve) and normal distributions (smooth curves) for the mean value $m = 100$. The normal distribution is given for two values of the width parameter σ_w which is shown in the text to be equal to the standard deviation σ. The Poisson distribution approximates well the normal distribution if the latter has $\sigma = \sqrt{m}$. Note the slight asymmetry of the Poisson distribution relative to the normal distribution. The standard deviation and full width half maximum widths are shown for the higher normal peak; the two normal curves happen to cross at the FWHM point.

Normal distribution, Gaussian:

σ_w - a characteristic width:

$x = m \pm \sigma_w$
the function has fallen to:

$e^{-0.5} = 0.601$

of its maximum value.

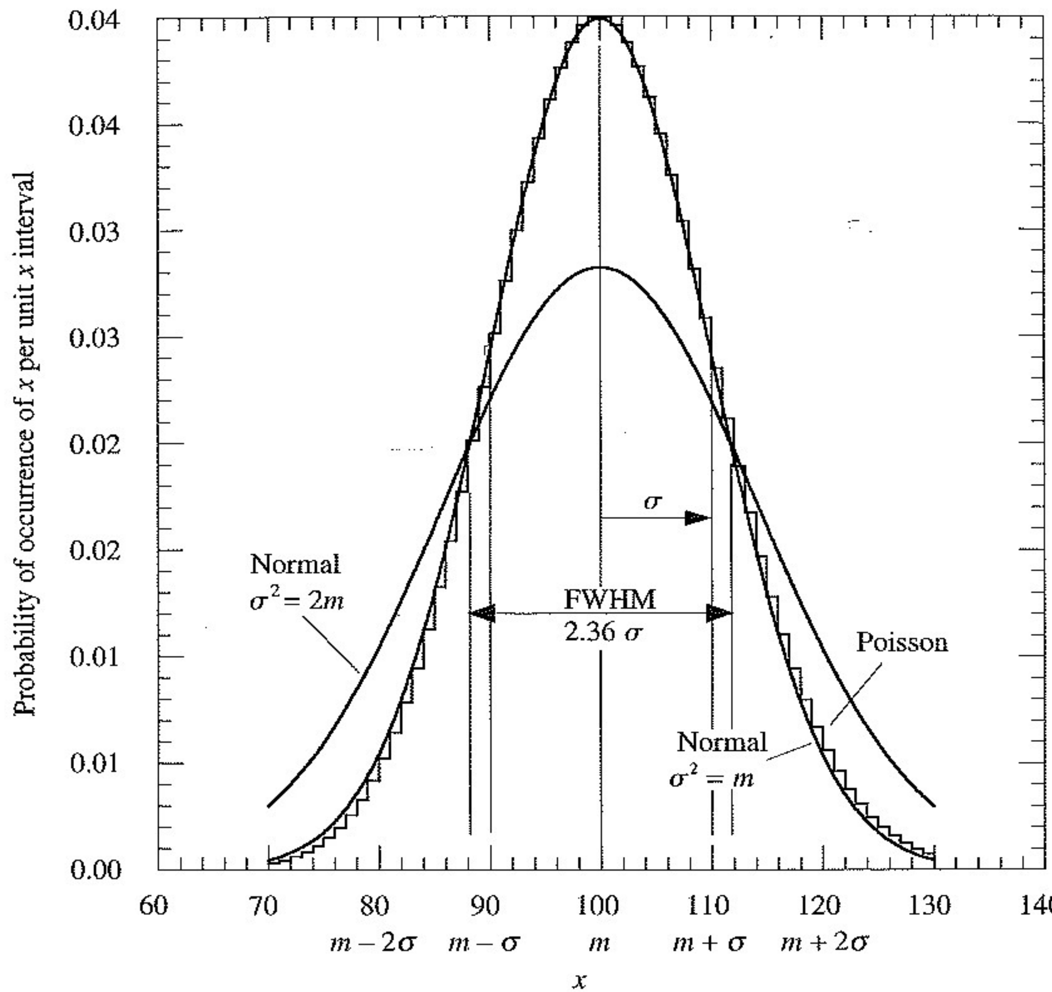

Figure 6.8. The Poisson (step curve) and normal distributions (smooth curves) for the mean value $m = 100$. The normal distribution is given for two values of the width parameter σ_w which is shown in the text to be equal to the standard deviation σ. The Poisson distribution approximates well the normal distribution if the latter has $\sigma = \sqrt{m}$. Note the slight asymmetry of the Poisson distribution relative to the normal distribution. The standard deviation and full width half maximum widths are shown for the higher normal peak; the two normal curves happen to cross at the FWHM point.

Normal distribution, Gaussian:

σ_w - a characteristic width:

$$x = m \pm \sigma_w$$

the function has fallen to:

$$e^{-0.5} = 0.601$$

of its maximum value. For:

$$x - m = \sqrt{2}\,\sigma_w$$

$$e^{-1} = 0.37$$

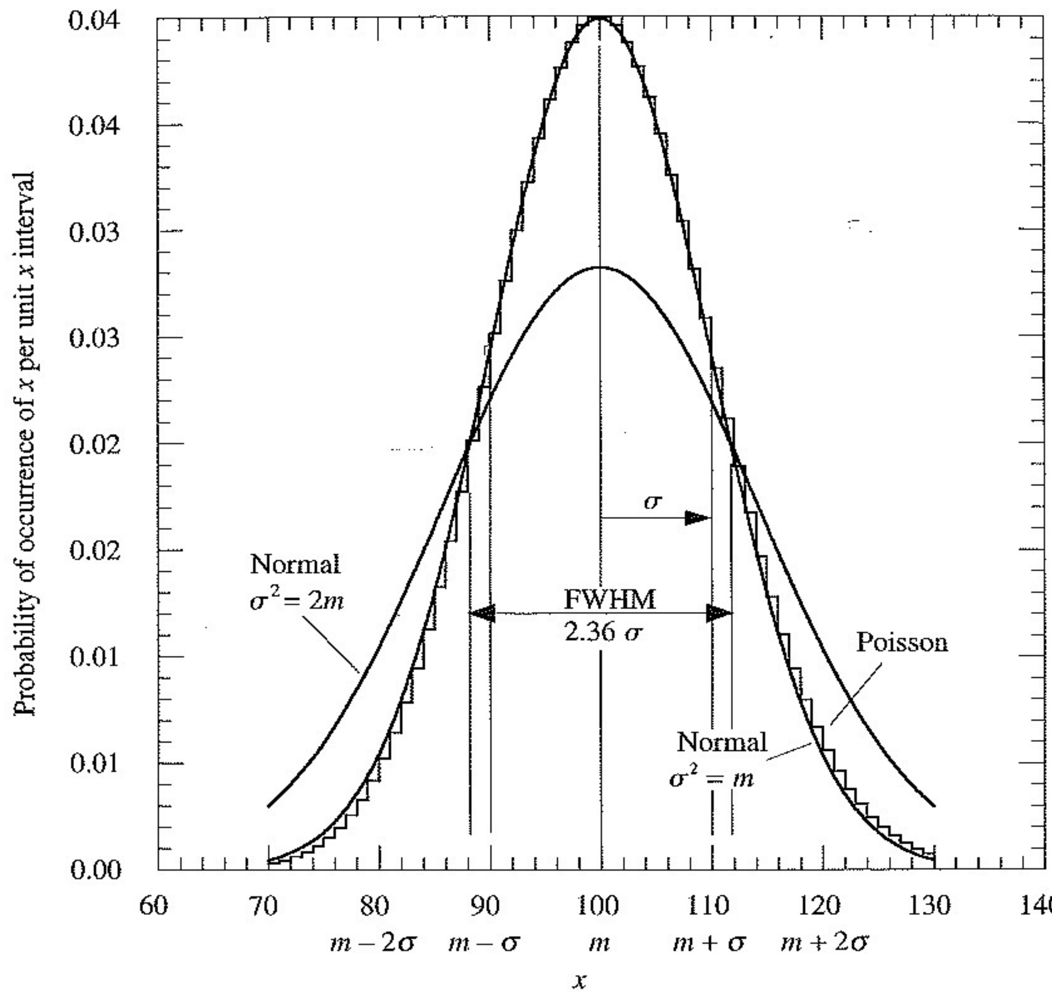

Figure 6.8. The Poisson (step curve) and normal distributions (smooth curves) for the mean value $m = 100$. The normal distribution is given for two values of the width parameter σ_w which is shown in the text to be equal to the standard deviation σ. The Poisson distribution approximates well the normal distribution if the latter has $\sigma = \sqrt{m}$. Note the slight asymmetry of the Poisson distribution relative to the normal distribution. The standard deviation and full width half maximum widths are shown for the higher normal peak; the two normal curves happen to cross at the FWHM point.

Normal distribution, Gaussian:

- 68% of the area falls in 1 σ_w
- 95.5 % falls in 2 σ_w
- 99.73 % falls in 3 σ_w

from integrating eq. of distribution.

Table 6.2. *Normal distribution probabilities*

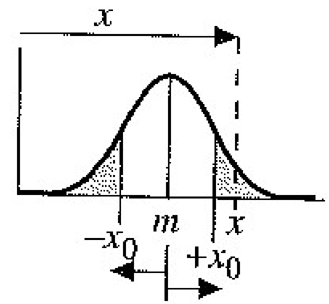

$\left(\frac{x_0}{\sigma}\right)^a$	Area (shaded) at $\lvert x - m \rvert > x_0$ [b]	$\left(\frac{x_0}{\sigma}\right)^a$	Area (shaded) at $\lvert x - m \rvert > x_0$ [b]
0	1.00	2.5	0.0124
0.5	0.617	3.0	0.00270
1.0	0.317	3.5	4.65×10^{-4}
1.2	0.230	4.0	6.34×10^{-5}
1.4	0.162	5.0	5.73×10^{-7}
1.6	0.110	6.0	2.0×10^{-9}
1.8	0.0719	7.0	2.6×10^{-12}
2.0	0.0455		

[a] Ratio of deviation x_0 to standard deviation σ. The standard deviation σ is equal to σ_w, the width parameter of the distribution.
[b] Probability of occurrence of deviation greater than $\pm x_0$.

Normal and Poisson distribution:

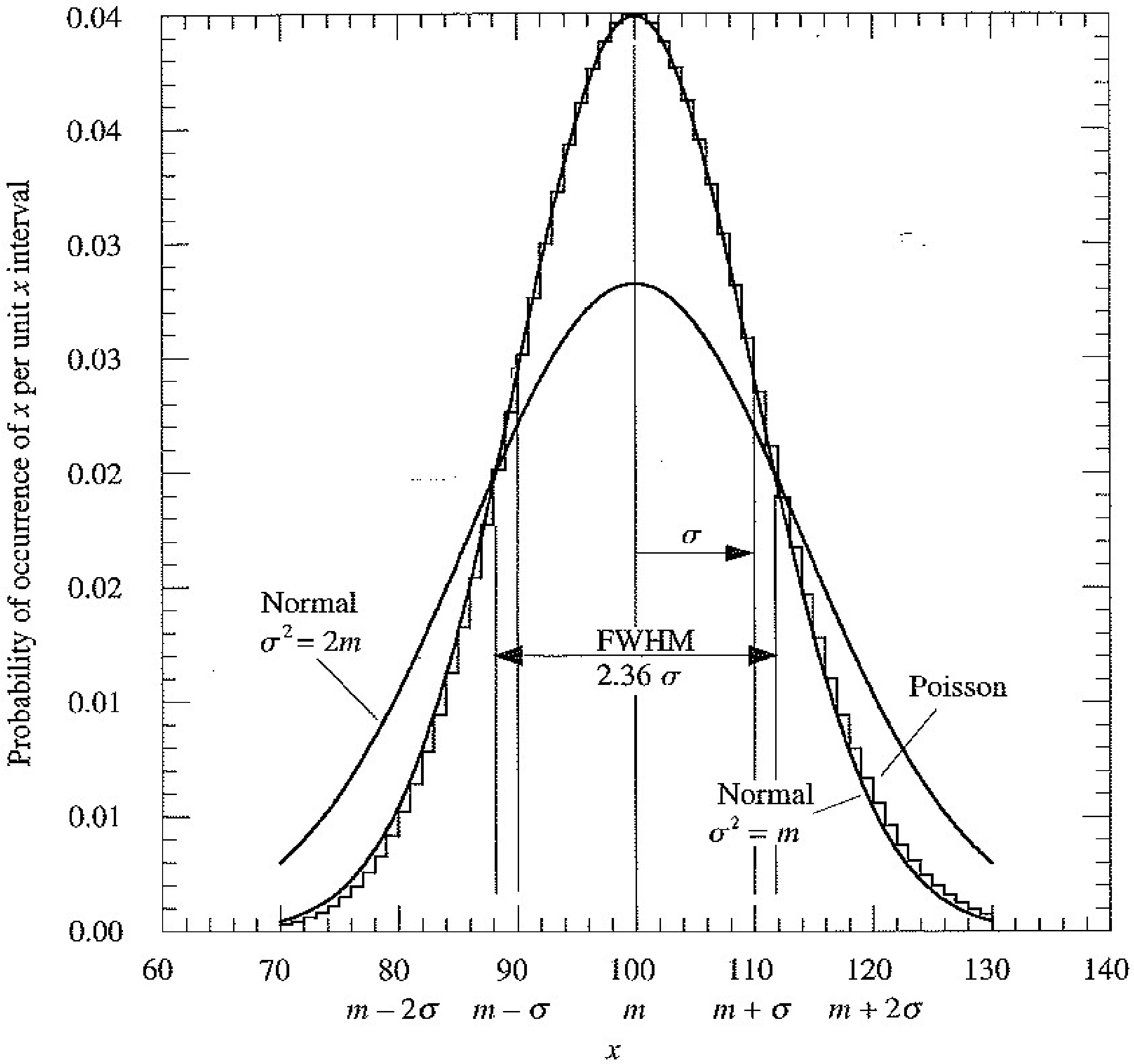

For large values of *m*, the Poisson distribution approaches in shape the central part of the normal distribution if the width parameter is set to:

$$\sigma_w = m^{1/2}$$

Normal distribution describes the arrival of random events for large m.

Variance and standard deviation:

The width of a *measured* distribution indicates the range of values obtained from a set of individual measurements of *x*. Formally *root-mean-square deviation*, i.e. *standard deviation,* σ , its square is called the *variance*:

$$\sigma^2 = \frac{1}{n} \sum_{i=1}^{i=n} (x_i - m)^2$$

definition of variance.

n – number of independent measurements,
x_i – individual measurements,
m – mean value can be only obtained with an infinite amount of data !!!

Variance and standard deviation:

In practice the average value x_{av} of the n measured numbers may be the best approximation of m that is available:

$$\sigma^2 = \frac{1}{n-1} \sum_{i=1}^{i=n} (x_i - x_{av})^2$$

practical variance.

Practical variance equals theoretical for large n.

Variance and standard deviation:

In practice the average value x_{av} of the n measured numbers may be the best approximation of m that is available:

$$\sigma^2 = \frac{1}{n-1} \sum_{i=1}^{i=n} (x_i - x_{av})^2$$

practical variance.

Practical variance equal theoretical for large n.

Variance can be evaluated for any given experimental distribution as Poisson or Normal.

Variance and standard deviation:

Variance of theoretical Poisson distribution:

n_j – occurrences of the same value x_j,

It is useful to rewrite variance in terms of the probability used in theoretical expression: Summation will be over *x*, than the trial number *j*.

$$\sigma^2 = \sum_{j=1}^{j=n} (x_j - m)^2 \frac{n_j}{n} = \sum_{x=-\infty}^{x=\infty} (x-m)^2 P_x, \qquad \left(x_{av} = \sum_{j=1}^{j=n} \frac{x_j}{n} \right)$$

Variance and standard deviation:

Variance of theoretical Poisson distribution:
n_j – occurrences of the same value $x_{j,}$
It is useful to rewrite variance in terms of the probability used in theoretical expression. Summation will be over *x*, than the trial number *j*.

$$\sigma^2 = \sum_{j=1}^{j=n} (x_j - m)^2 \frac{n_j}{n} = \sum_{x=-\infty}^{x=\infty} (x-m)^2 P_x, \qquad \left(x_{av} = \sum_{j=1}^{j=n} \frac{x_j}{n} \right)$$

Substituting the Poisson distribution:

$$\sigma^2 = \sum_{x=-\infty}^{x=\infty} \frac{(x-m)^2 m^x e^{-m}}{x!} = m,$$

$$\sigma_w = m^{1/2}$$

Example:

If 100 photons are expected to arrive at pixel of a CCD during exposure of 1s, standard deviation for a single measurement is:

$$\sigma = \sqrt{100} = 10$$

We can expect fluctuations ± 10 or even ± 30 about the 100 count mean.

Example:

If 100 photons are expected to arrive at pixel of a CCD during exposure of 1s, standard deviation for a single measurement is:

$$\sigma = \sqrt{100} = 10$$

We can expect fluctuations ±10 or even ±30 about the 100 count mean.
The uncertainty relative to the mean value is:

$$\sigma / m = 10/100 = 10\%$$

It is “a 10% measurement”. If in 100 s, one expect 10000 counts:

$$\sigma = \sqrt{10000} = 100, \quad \sigma / m = 100/10000 = 1\%$$

More counts leads to higher absolute fluctuations and uncertainty, but fractional uncertainty is reduced. Longer means better rates.

Variance and standard deviation:

Variance of Normal distribution is obtained through substitution of sum into integral form:

$$\sigma^2 = \int_{x=-\infty}^{x=\infty} (x-m)^2 \, dP_x$$

$$\sigma^2 = \frac{1}{\sigma_w \sqrt{2\pi}} \int_{x=-\infty}^{x=\infty} (x-m)^2 \exp\left[\frac{-(x-m)^2}{2\sigma_w^2}\right]$$

$$\sigma^2 = \sigma_w^2$$

Measurement significance:

For large number of events $\sigma = m^{1/2}$

The probability of exceeding 3 sigma is 0.27%.
If the pixel of CCD is expected to record 100 photons during the exposure time thus $\sigma = 10.$

If we measure 130 photons, we may ask, is it bright source or fluctuation? This is 3 sigma detection, but still there is one chance in 1/(0.0027)=370 that this would happen from statistical fluctuations.

One measures of 5 sigma error in one of measurements. The probability of a statistical fluctuations in one given trial is 6 x 10-7, but CCD has 4 million pixels, thus:

$$expectation\, value = 6 \times 10^{-7} \times 4 \times 10^{6} = 2.4$$

<u>Background:</u>

• Counts due to cosmic rays particles – anticoincidence logic.
• Counts due to diffuse X-ray background.

Commonly, two measurements will be made:
1) one with astrophysical source in the field of view,
2) one with offset from the source to measure bkgr only.

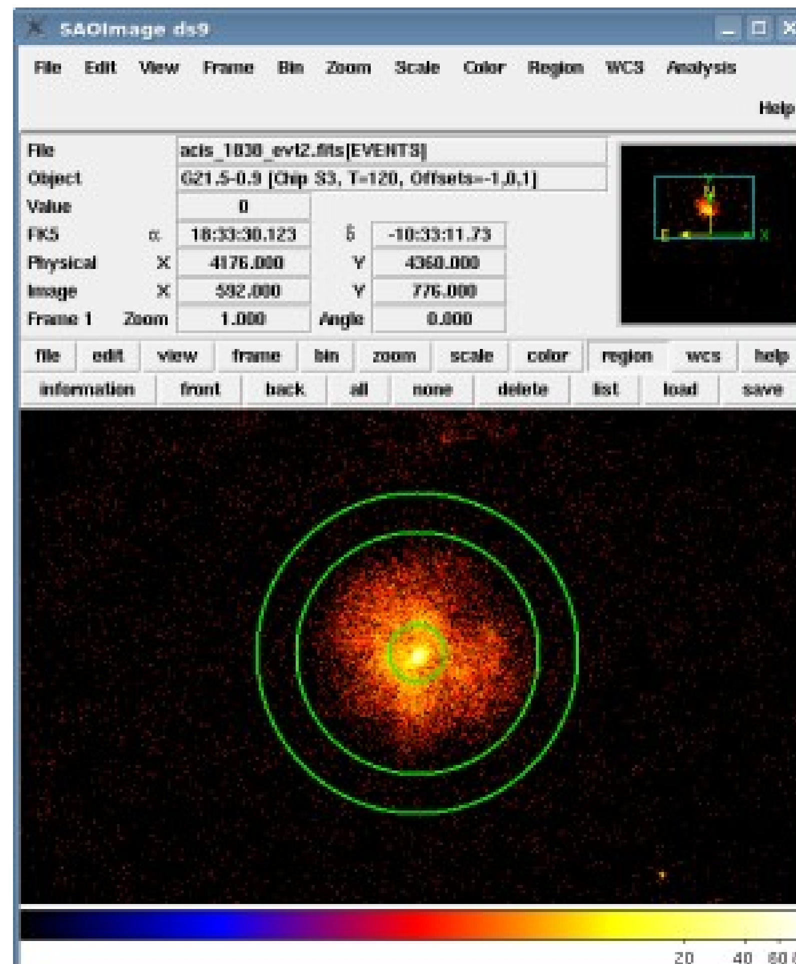

If the detector/telescope produces a sky image, we can make both measurements in a single exposure.

Propagation of errors:

After data are taken, one invariably manipulates then to obtain other quantities:

$$\frac{\text{accumulated number of counts}}{\text{accumulated time}} = \text{rate of photon arrival}$$

Propagation of errors:

After data are taken, one invariably manipulates then to obtain other quantities:

$$\frac{\text{accumulated number of counts}}{\text{accumulated time}} = \text{rate of photon arrival}$$

Assume, x and y be a length, each accurate to 1mm:

$$z = x + y, \qquad z = x - y$$

$$dz = dx + dy$$

$$|dz|_{max} = |dx|_{max} + |dy|_{max}$$

Maximum error is thus a sum of the individual maximum errors.

Propagation of errors:

Assume, x and y be a length, each accurate to 1mm:

$$z = x * y, \qquad z = x / y$$

Fractional error is the sum of the individual fractional errors:

or:

$$dz = x * dy + y * dx$$

$$|dz/z|_{max} = |dx/x|_{max} + |dy/y|_{max}$$

We assume to maximize the error. In fact the measurements of *x* and *y* would most likely be uncorrelated.

Fractional errors are thus, on average, less than the maximum values found above.

Propagation of errors:

If x and y vary independently with normal distribution, characterized by standard deviation,

error of summation or subtraction:

$$\sigma_z^2 = \sigma_x^2 + \sigma_y^2$$

$$x = y \quad \Rightarrow \quad \sigma_z = \sqrt{2}\,\sigma_x$$

$$x > y \quad \Rightarrow \quad \sigma_z \approx \sigma_x$$

error in a product or quotient:

$$\frac{\sigma_z}{z}^2 = \frac{\sigma_x}{x}^2 + \frac{\sigma_y}{y}^2$$

Background subtraction:

S – expected number of counts detected in Δt time interval,

B – expected number of counts of bkgr in the same time interval.

ON Source – $S+B$,
OFF Source – B.

Background subtraction:

S – expected number of counts detected in *Δt* time interval,

B – expected number of counts of bkgr in the same time interval.

ON Source – *S*+*B*,
OFF Source – *B*.

Signal counts; equal exposures:

$$S = (S + B) - B$$

Two measurements are quite independent: different photons and different bkgr are involved. Thus the fluctuation will be uncorrelated:

$$\sigma_s^2 = \sigma_{s+b}^2 + \sigma_b^2$$

Background subtraction:

Two standard deviations obtained from the Poisson distribution:

$$\sigma_s^2 = S + B + B = S + 2\mathrm{B}$$

$$\sigma_s \ll S \quad \Rightarrow \quad \textit{high quality of measurement},$$

$$S = 3\sigma_s \quad \Rightarrow \quad 3\sigma \quad \textit{result},$$

$$S < 3\sigma_s \quad \Rightarrow \quad \textit{detection questionable}.$$

Background subtraction:

Significance equals number of standard deviations or S/N:

$$\frac{S}{\sigma_s} = \frac{S}{\sqrt{S+2B}} \qquad \text{signal-to-noise ratio} .$$

Background subtraction:

Significance equals number of standard deviations or S/N:

$$\frac{S}{\sigma_s} = \frac{S}{\sqrt{S + 2B}} \qquad \text{signal-to-noise ratio.}$$

The intensity of the source is best represented by the source event rate r_s (counts/s). With equal on-source and off-source accumulated time Δt :

$$r_s = \frac{S}{\Delta t} \qquad r_b = \frac{B}{\Delta t}$$

Low and high background limits:

The low-background (B<<S) case gives:

$$\frac{S}{\sigma_s} \approx \frac{S}{\sqrt{S}} = \sqrt{S} = \sqrt{r_s \Delta t}$$

bkgr negligible

Significance increases as the square root of the number of counts.

To increase significance to 5 sigma – to increase duration time by a factor of $(5/2)^2=6.25$.

Low and hight background limits:

The low-background (B<<S) case gives:

$$\frac{S}{\sigma_s} \approx \frac{S}{\sqrt{S}} = \sqrt{S} = \sqrt{r_s \Delta t}$$

bkgr negligible

Significance increases as the square root of the number of counts.
To increase significance to 5 sigma – to increase duration time by a factor of $(5/2)^2=6.25$.

The high-background (B>> S) case gives:

$$\frac{S}{\sigma_s} \approx \frac{S}{\sqrt{2B}} = \frac{r_s \Delta t}{\sqrt{2 r_b \Delta t}} = \frac{r_s}{\sqrt{2 r_b}} \sqrt{\Delta t}$$

bkgr dominates.

It takes a lot of observing time to increase significance.

Low and hight background limits:

Let us compare the S/N ratios of two hypothetical detectors, one *high-B* and the other of *low-B*.

Comparison of two sensitivities:

$$\left(\frac{S}{\sigma_s}\right)_{B\gg S} = \sqrt{\frac{r_s}{2r_b}}\left(\frac{S}{\sigma_s}\right)_{B\ll S}$$

Since $r_s << r_b$, the expression tells us that the significance is much less in the high-B case than for the low-B case for similar exposures.

Bright and faint source observations:

Focusing instruments are low-B systems.
3 X-rays photons in one resolution element of the focal plane could be highly significant since bkgr so low.

If the expected bkgr in the element is only 0.1 counts, the probability of this bkgr giving rise to the 3 X-rays is:

$$P_x = \frac{m^x e^{-m}}{x!} = \frac{0.1^3 e^{-0.1}}{3!} = 1.5 \times 10^{-4}$$

Focusing instruments – the best for faint sources.

Bright and faint source observations:

How does the significance of a detection in a given time depends on source intensity i.e., on the rate r_s.

When S>B as in focusing instruments, the statistical noise arises from the source itself.

$$S \quad increases \quad \Rightarrow \quad Statistical \quad noise \quad increases$$

$$\frac{S}{\sigma_s} \quad increases\, slowly\, with \quad \sqrt{r_s}$$

($S/\sigma_s \approx \sqrt{r_s \Delta t}$ **for low-B)**

Bright and faint source observations:

How does the significance of a detection in a given time depends on source intensity i.e., on the rate r_s.

When S>B as in focusing instruments, the statistical noise arises from the source itself:

$$S \quad increases \quad \Rightarrow \quad Statistical \quad noise \quad increases$$

$$\frac{S}{\sigma_s} \quad increases\,slowly\,with \quad \sqrt{r_s}$$

($S/\sigma_s \approx \sqrt{r_s \Delta t}$ **for low-B)**

When S<B: $$\frac{S}{\sigma_s} \quad increases\,with \quad r_s$$

($S/\sigma_s \approx r_s / \sqrt{2 r_b} \cdot \sqrt{\Delta t}$ **for high-B)**

source with twice intensity will be measured with twice the significance, statistical noise depends only on the bkgr rate.

Bright and faint source observations:

$$\left(\frac{S}{\sigma_s}\right)_{B \gg S} = \sqrt{\frac{r_s}{2r_b}} \left(\frac{S}{\sigma_s}\right)_{B \ll S}$$

They can differ by:
-effective area
-different energies control.

For example non-focusing high-B X-ray detector, PC & MC has large collecting area A, is sensitive up to 60 keV.

Focusing low-B reaches only about 8 keV. A_eff << A_coll.

For bright sources, a high-B large area system can yield a higher significance (S/N) in a given time that can a low-B system.

The Rossi X-ray Timing Explorer (RXTE)
low E and ang. resolution, great timing accuracy.

Bright and faint source observations:

$$\left(\frac{S}{\sigma_s}\right)_{B \gg S} = \sqrt{\frac{r_s}{2r_b}}\left(\frac{S}{\sigma_s}\right)_{B \ll S}$$

They can differ by:

- *-effective area*
- *-different energies control.*

$$\frac{r_s}{r_b} \quad \text{increases but still well} \ll 1$$

The sensitivity of high-B detector moves toward the sensitivity of low-B detector.

The adventure of the low-B detector decreases as the source brightens.

When source becomes so bright in the high-B detector that it exceeds its high bkgr, the weak-bkgr limit applies to both detectors.

Homework #5: Writing exercise (old style):

1) The magnitude of the charge pulse from proportional counter fluctuates in value from one incident X ray to another, even when the incident X rays all have the same energy, E, those obtained from iron 55 radioactive source.

a) Consider the detection of 6.0 keV X-rays in an argon- filled PC. What is the standard deviation in the units of keV of these fluctuations if they arise mostly from Poisson fluctuations in a number of ion pairs created by the initial photo-electrons? Assume that these are no escape photons, and consider only the first generation of ion pairs, those created by the several initial photo-electrons with a combined energy of 6.0 keV. What is the fractional energy resolution defined as the FWHM of the response curve divided by the mean energy, at this X-ray energy?

b) What are the fractional energy resolutions at energies 2 keV and 30 keV?

NEXT LECTURE on Dec. 8th 2022

- Overview of HW#3 and #4

- data to practice are:

wi-fi password: a w sercu maj
We have eduroam as well